

## Abstract

Title of Thesis: STAGE III N-SATURATED FORESTED WATERSHED  
RAPIDY RESPONDS TO DECLINING ATMOSPHERIC N  
DEPOSITION

Robert D. Sabo, Master of Science, 2014

Thesis directed by: Professor Keith N. Eshleman  
University of Maryland Center for Environmental Science

This study used a mass balance approach by characterizing the input, output, and sink rates of N in order to assess a declared “stage III N-saturated forest” response to decreased atmospheric N deposition in western Maryland. Relying on the conceptual model of kinetic N-saturation to holistically link stream, vegetative, soil, and atmospheric compartments and the use of the novel  $\Delta^{17}\text{O}$  isotopic technique, the study demonstrated dynamic soil  $\text{NO}_3\text{-N}$  pools, unprocessed atmospheric  $\text{NO}_3\text{-N}$  in base flow, and significant reductions in  $\text{NO}_3\text{-N}$  yield in response to decreased atmospheric N deposition. A lumped conceptual model, incorporating a dormant season  $\text{NO}_3\text{-N}$  flush, was proposed that explains forest response to decreased deposition and sheds light on the hydrologic processes that govern the storage/release of  $\text{NO}_3\text{-N}$  among years. It is proposed that this flushing mechanism prevents forests from attaining higher stages of N-saturation and predicts forests will be responsive to further reductions in N deposition.

STAGE III N-SATURATED FORESTED WATERSHED RAPIDLY RESPONDS TO  
DECLINING ATMOSPHERIC N DEPOSITION

by

Robert D. Sabo

Thesis submitted to the Faculty of the Graduate School of the  
University of Maryland, College Park, in partial fulfillment  
of the requirements for the degree of  
Master of Science  
2014

Advisory Committee

Professor Keith N. Eshleman  
Associate Professor Andrew Elmore  
Assistant Professor David Nelson

## Table of Contents

Figure List.....	iii
Table List .....	iv
Introduction.....	1
Methods.....	8
Site Location, Age, Past Demography, Land-Use History, and Soil .....	8
Stream water discharge and N fluxes.....	10
Isotopic Analysis.....	12
Soil Analyses .....	14
Kinetic N-Saturation Model.....	17
Results.....	23
Atmospheric Deposition .....	23
Hydrology .....	24
Streamwater N Yields and Concentrations .....	26
Stable Isotope Analysis.....	27
Soil Net N Fluxes and Pools .....	33
Kinetic N-saturation Model .....	37
Discussion.....	42
Application of the Expanded Modified Kinetic N Saturation Model .....	52
Appendix.....	56

Literature Cited ..... 75

### Figure List

Fig. 1 Map of the TNEF watershed with the permanent sampling plots and permanent transects..... 9

Fig. 2 Annual total atmospheric deposition (wet+dry) at TNEF from 1986-2011. Total deposition was calculated by combining modeled wet deposition rates from NADP/PRISM areal extracted values with reported dry deposition rates from a nearby NADP site at Laurel Ridge, PA. Linear regression was significant ( $P < 0.0001$ ). ..... 24

Fig. 3 Monthly flow-weighted concentrations and yields of  $\text{NO}_3\text{-N}$  along with monthly runoff values for the 2012 and 2013 water year at TNEF. .... 26

Fig. 4 Atmospheric and processed  $\text{NO}_3\text{-N}$  concentrations, error bars represent maximum and minimum range of atmospheric and processed concentrations. Instantaneous discharge values (15-minute data) are also shown. .... 28

Fig. 5 Total (left y-axis), processed (left y-axis), and atmospheric  $\text{NO}_3\text{-N}$  (right y-axis) concentrations following the hurricane Sandy episode in late October water year 2013. The bottom figure displays the  $\text{NO}_3\text{-N}$   $\delta^{15}\text{N}$  signature throughout the event. .... 31

Fig. 6 Atmospheric and processed monthly flow-weighted average  $\text{NO}_3\text{-N}$  concentrations, monthly yields, and monthly runoff. .... 32

Fig. 7 Relationship between processed streamwater  $\text{NO}_3\text{-N}$  concentrations and their associated  $\delta^{15}\text{N}$  signal within  $\text{NO}_3\text{-N}$ . Linear regression was significant ( $P < 0.0001$ ). .... 32

Fig. 8 Standing pools of inorganic nitrogen within the top 10 cm of soil during the 2012 growing season and May 2013 (following the dormant season flush) with standard error bars. \*Refer to Methods for details on the computation of November values. .... 33

Fig. 9 Mean monthly pools of inorganic nitrogen within the top 10 cm of soil during the 2012 growing season and May 2013 following the dormant season flush. .... 34

Fig. 10 Mean net vegetative IN uptake rates (top) within the Oe/Oa horizon and top 10 cm of mineral soil during the 2012 growing season. Net mineralization rates (bottom) are segmented into net NH<sub>4</sub>-N and NO<sub>3</sub>-N production rates within the Oe/Oa and lower mineral horizon. .... 35

Fig. 11 Theoretical yield of total, atmospheric, and processed NO<sub>3</sub>-N yield based on estimated parameters for TNEF ( $a=0.1$  and  $M=70 \text{ kg ha}^{-1} \text{ yr}^{-1}$ ). Processed, atmospheric, and total yield determined by eq 18-20..... 38

Figure 12 Modeled (eq. 20) and measured yields of total, atmospheric, and processed NO<sub>3</sub>-N from TNEF. Estimated model parameters,  $a=0.1$  and  $M=70 \text{ kg ha}^{-1} \text{ yr}^{-1}$  ..... 38

Figure 13. Decline in monthly soil NO<sub>3</sub>-N pools throughout the course of the dormant season of water year 2013. Losses from the soil pools are attributed to the flush of NO<sub>3</sub>-N, which is described by the monthly stream yields of atmospheric and processed NO<sub>3</sub>-N. .... 49

Figure A 1. Atmospheric NO<sub>3</sub>-N concentrations (blue dots), and processed NO<sub>3</sub>-N concentrations (red dots) at two month intervals. Error bars represent maximum and minimum range of atmospheric and processed concentrations. Instantaneous discharge values (15-minute data) are also shown (black lines).(pp. 66-68) ..... 56

**Table List**

Table 1 Volume-weighted annual concentration of inorganic nitrogen in precipitation and annual wet deposition rates of inorganic nitrogen at TNEF on a water year basis. Dry deposition estimates are on a calendar year basis. .... 23

Table 2 Annual flow-weighted average concentrations of NO<sub>3</sub>-N, DON, IN, IN retention (IN annual yield/ Total IN Deposition), evapotranspiration (ET), and runoff for the TNEF watershed for 2000-2004 and 2012-2013 water years. Data for water years 2000-2004 from Castro et al. (2007) was adjusted to reflect use of 4 ha watershed area..... 25

Table 3. Rates of net N mineralization, net nitrification, and nitrification to mineralization ratios for water year 2012. Comparable data from 2000 and 2002 from Castro et al. (2007)..... 37

Table 4. Results from the application of the alternate yield model (eq 16-18) relying solely on N-flux field measurements from water year 2012. Yield columns display

predicted and observed (*italics*) values. Measured constants for *M*, *D*, *Pa*, and *Pp* are 86, 5.68, 0.06, and 0.94, respectively. .... 40

Table A 1. Displays monthly net mineralization and nitrification rates, nitrification to mineralization ratios, and annual rates within Oe/Oa and mineral horizons at TNEF for WY 2012..... 59

Table A 2. Monthly standing pools of NH<sub>4</sub>-N, NO<sub>3</sub>-N, and IN within the Oe/Oa and mineral horizons at TNEF for WY 2012. .... 60

Table A 3. Monthly fluxes of NH<sub>4</sub>-N, NO<sub>3</sub>-N, and IN within the top ten cm of mineral soil at TNEF for WY 2012..... 61

Table A 4. Seasonal loads (kg ha<sup>-1</sup> yr<sup>-1</sup>) and depth-weighted concentrations (mg N L<sup>-1</sup>) of NH<sub>4</sub>-N, NO<sub>3</sub>-N, TN and IN from precipitation at TNEF for WY 2012-2013. .... 62

Table A 5. Monthly runoff, yields and volume-weighted concentrations of NH<sub>4</sub>-N, NO<sub>3</sub>-N, and DON from the stream at TNEF for WY 2012-2013. .... 63

Table A 6. Monthly runoff, yields and volume-weighted concentrations of atmospheric and processed NO<sub>3</sub>-N ( $\Delta O17=20$ ) from the stream at TNEF for WY 2012-2013. .... 64

Table A 7. Monthly runoff, yields and volume-weighted concentrations of atmospheric and processed NO<sub>3</sub>-N ( $\Delta O17=30$ ) from the stream at TNEF for WY 2012-2013. .... 65

Table A 8. Grab sample concentration (mg N L<sup>-1</sup>) from the stream at TNEF for WY 2012-2013. .... 66

Table A 9. Isotopic signatures for NO<sub>3</sub>-N from the stream at TNEF for WY 2012-2013, along with calculated atmospheric and processes proportions present in the total NO<sub>3</sub>-N concentration..... 68

Table A 10. Monthly net nitrification and mineralization rates (g m<sup>-2</sup> mo<sup>-2</sup>) within the the top 10 cm of mineral soil at TNEF. Sections are split up by months and have subsection that display within and inter-plot variability. FF stands for Oe/Oa horizon..... 71

Table A 11. Results generated from the spring sampling isotopic approach (eq. 22)  
relying on the March 22, 2013 spring stream sample and annual IN  
concentration/deposition data from water year 2012..... 74

## **Introduction**

Impaired water quality compromises the rich cultural, recreational, and ecological services of the Chesapeake Bay (Boesch et al. 2001). Persistent eutrophic conditions exist in the estuary, due to excessive nitrogen and phosphorus yields transported from its watershed to the estuary (Boesch et al. 2001). These nutrient subsidies contribute to the formation of harmful/toxic algal blooms and dead zones, which ultimately endanger fisheries and public health (Castro and Driscoll 2002; Pan et al. 2004). The United States Environmental Protection Agency and states that fall within the watershed boundaries of the Chesapeake Bay are currently developing localized watershed implementation plans (WIPS) in order to meet targeted surface water quality goals (EPA 2010). Local municipalities are developing strategies that utilize a suite of best management practices, ranging from costly infrastructure improvements to riparian buffer plantings, to meet federally established total maximum daily yields for phosphorus, nitrogen, and suspended solids (EPA 2010).

Under current Phase 5.3 Watershed Model scenarios that have informed WIPS development for the 2010 total maximum daily yields, forests are not thought to have significantly contributed to the modeled decrease in N export to the Bay over the past three decades (Shenk and Linker 2013). The bulk of the declines in N export to the Bay are attributed to agricultural best management practices, cuts in atmospheric N deposition, and wastewater treatment plant upgrades (Shenk and Linker 2013). These modeled improvements are supported by observations of declining NO<sub>3</sub>-N export at long-term monitoring stations along major tributaries (Hirsch et al. 2010); however, the



allocations of improvements may be misattributed in light of recent reports of forests rapidly responding to decreased atmospheric N deposition (Eshleman et al. 2013).

Multiple studies have reported rapid decreases in N export from forested watersheds coincident with significant reductions in atmospheric N deposition (Wright et al. 1993; Corre and Lamersdorf 2004; Kothawala et al. 2011; Waller et al. 2012; Eshleman et al. 2013). The  $\text{NO}_3\text{-N}$  export from pre-dominantly forested watersheds in the central Appalachians have decreased by 40-70% since 1986, with declines beginning in 1997 when implementation of  $\text{NO}_x$  emission standards for power plants were enforced under the Clean Air Act Amendments of 1990 (Eshleman et al. 2013). It is possible that a significant fraction of the modeled and observed declines in N yields to the Chesapeake Bay could be attributed to declines in forest N export since forests are the predominant land use in the watershed at ~60% (EPA 2010). The observation of forested watersheds rapidly responding to decreased atmospheric N inputs is perplexing in light of our current conceptual understanding of forest N biogeochemistry.

The “Staged N-Saturation Hypothesis” is a widely accepted model of forest N biogeochemistry; it takes a symptomatic approach to describing N-flux in forested ecosystems and proposes a mechanism that predicts forest experiencing chronic N deposition over time will become enriched in N within the organic pools in soils (Aber et al. 1998; Ågren and Bosatta 1988). This hypothesis states that forests progress through stages of N-saturation that can be identified by observations of predictable symptoms such as low C:N ratios in soils,  $\text{NO}_3\text{-N}$  leaching, net nitrification, and increased N mineralization (Aber et al. 1998). The N-status of the forested ecosystem is predicted to change, fueling elevated net nitrification and mineralization rates that make inorganic N

(IN) vulnerable to leaching during the dormant season (Galloway et al. 2003). Utilizing space for time methods, researchers have asserted that forest N retention is determined by the accumulative rate of deposition, which implicitly predicts that forests will slowly respond to declining N deposition (Aber et al. 2003). These recent observations of declining N export from forested watersheds along with results from European NITREX studies have demonstrated a need to refine our understanding of forest biogeochemistry (Bredemeier et al. 1995; Eshleman et al. 2013; Kothawala et al. 2011).

An alternative model of the relationship between forest N processes and atmospheric N deposition is the kinetic N saturation model proposed by Lovett and Goodale (2011). The kinetic N saturation model takes a non-symptomatic mass balance approach that focuses on the input, output, and sink rates of N in temperate forested ecosystems. Rather than describing the temporal patterns of N cycling indicators as in the staged N saturation model, the kinetic N saturation model focuses on the dynamics of the soil IN pools and its interactions with atmospheric, soil, vegetation, and stream compartments of a temperate forest ecosystem. The N mass balance is described below in equation 1:

$$D - V - S = Y + G$$

(1)

In equation 1,  $D$  is N deposition,  $V$  is net incorporation of N into vegetation,  $S$  is net incorporation into soil,  $Y$  is the yield or export of N to surface waters, and  $G$  is the gaseous N loss. Assuming that  $V$  and  $S$  are relatively constant, this mass balance predicts forests would not attain higher stages of N saturation, since any excess N not incorporated into the vegetation and soil compartments is fluxed out of the system

through stream or gaseous loss. One important implication of the proposed kinetic N saturation model is that forest N yields are dynamic and would be expected to rapidly respond to changes in atmospheric N deposition.

An example of this rapid response was reported by Eshleman et al. (2013), who made the net sink rates of the kinetic N saturation model a linear function of  $D$ , and in doing so explained declining  $\text{NO}_3\text{-N}$  trends in nine pre-dominantly forested watersheds (1-10,000  $\text{km}^2$ ) throughout the central Appalachians. By combining the  $S$  and  $V$  term into a net accumulation term  $A$ , neglecting  $G$ , and making  $A$  linear function of  $D$ , they produced empirically derived retention coefficients ( $0 \leq a \leq 1$ ) through a modified kinetic N saturation model.

$$Y = D - aD$$

(2)

These retention coefficients were not found to be determined by the input rate “ $D$ ” rather they were inherent to the particular watershed based on regional and site specific drivers. Essentially the study demonstrated that the net accumulation and  $\text{NO}_3\text{-N}$  yields of forests were proportionally responsive to the rate of inputs on an annual basis. The results also suggested that short term intra-annual variation in soil and vegetation processes cannot be the major drivers of the observed trends in  $\text{NO}_3\text{-N}$  yields. Though powerful in confirming the utility of the kinetic N saturation concept, the authors did not propose the mechanism of forest response to declining atmospheric N deposition.

In establishing the mechanism of response, it is first imperative to state that few forests have displayed symptoms of extreme N saturation. This observation suggests that the integration of abiotic and biotic interactions within the ecosystem prevent the

majority of forests from progressing to higher stages of N saturation. These relatively steady state conditions, further revealed by the observation of Redfield like ratios for forests throughout the “globe” indicate that current levels of deposition do not overwhelm mechanisms that promote relatively constant C:N:P ratios in temperate forest soils and microbes (McGroddy et al. 2004; Cleveland and Liptzin 2007; Aber et al. 2003). This dynamic can be summarized through the mathematical concept of circular causal systems developed by Hutchinson (1948)<sup>1</sup>.

The circular paths are characterized well in the kinetic N saturation model which include dynamic NO<sub>3</sub>-N yields in streams (*Y*) and uptake or assimilation capacity by the vegetation and soil (*V* and *S*) in response to atmospheric N deposition (*D*). By holistically linking ecosystem compartments, this model avoids excessive reductionism and moves beyond the descriptive approach to forest biogeochemistry. Overall the symptoms of staged N-saturation once thought indicative of higher stages of N saturation (change in N status) could simply be manifestations of the operation of a circular causal system whose self-correcting limits have not been overwhelmed (Hutchinson 1948). For example, the commonly observed increase in net nitrification rates within “N-saturated” forest can simply be the reallocation of IN to an N species more vulnerable to being leached during the dormant season thus making the excess IN unavailable to the vegetation for the following growing season. This alternative interpretation raises the need to re-examine the dynamics of a stage-III N saturated forest over a longer time frame in order to

---

<sup>1</sup> “Such groups may be acted upon by their environment, and they may react upon it. If a set of properties in either system changes in such a way that the action of the first system on the second changes, this may cause changes in properties of the second system which alter the mode of action of the second system on the first.”

determine if the N-yield response can be explained by a kinetic N saturation model with an extremely low net accumulation potential (A).

The resulting stability (C:N:P ratios in soils) that circular causal paths create in ecosystems also makes interpretation difficult due to various processes operating and interacting within various timescales. Intra-annual variation in soil IN pools and stream IN export continuously fluctuate as these two ecosystem compartments interact throughout the year. The hydrology of the catchment, however, regulates the timing of IN delivery which drives the periodicity of the intra-annual variation seen in stream water yields and standing soil IN pools (Castellano et al. 2013). These intra-annual processes ultimately determine the inter-annual differences and interaction amongst years. Conventional annual mass balance approaches and long-term trend analysis may fail to capture these interactive processes amongst years, which may lead to improper dismissal of the local and regional drivers of N-flux.

The dismissal of atmospheric N deposition as a primary determinant of annual N yield in streams may be a prime example of inadequately linking forest ecosystem compartments at inter/intra-annual time scales (Bernal et al. 2012; Campbell et al. 2004; Goodale et al. 2003). In addition to the recent reports of forests rapidly responding to improved air quality, recent application of  $\Delta^{17}\text{O}$  isotopic analysis of  $\text{NO}_3\text{-N}$  has revealed significant fractions of unprocessed atmospheric  $\text{NO}_3\text{-N}$  present in soil, groundwater, and streamwater. This technique allows effective separation of the two different sources of  $\text{NO}_3\text{-N}$  (atmospheric/microbial) with the utilization of the conservative  $\Delta^{17}\text{O}$  atmospheric  $\text{NO}_3\text{-N}$  tracer, which is free from ecological fractionation biases that have been ascribed to dual isotopic analysis of  $\text{NO}_3\text{-N}$  (Fang et al. 2012; Michalski et al. 2004). In light of

these latest isotopic results and recent declining NO<sub>3</sub>-N trends coincident with decreased atmospheric deposition, it is asserted that variability in temperature and soil moisture conditions cannot solely drive stream NO<sub>3</sub>-N yield (Brookshire et al. 2011). Reductions in atmospheric N deposition are driving the observed trends because forest display relatively consistent retention factors over a range of deposition. The determination of these coefficients without long-term water quality records will be imperative for explaining the spatial variability of forest NO<sub>3</sub>-N inputs into streams and further identifying the proximal and distal drivers of N flux in temperate forest.

This study revisited a declared stage III N-saturated forest on the Appalachian Plateau in order to quantify its response to declining atmospheric N deposition and to establish if its response is consistent with regional observations (Castro et al. 2007; Eshleman et al. 2013). Basically, the five objectives of the project were to holistically link the coupled vegetation, nitrification, and mineralization complex with atmospheric N deposition in order to propose a conceptual model to explain regional observations reported by Eshleman et al. 2013. More specifically the objectives were:

- (1) *Establish the response of TNEF to declines in atmospheric N deposition by estimating its N input-output budget via traditional water quality monitoring techniques.*
- (2) *Analyze stable isotope composition of streamwater nitrate ( $\delta^{15}\text{N}$ ,  $\delta^{18}\text{O}$ , and  $\Delta^{17}\text{O}$ ) to establish a range of possible direct annual contributions of atmospheric nitrate to streamwater nitrate yield.*
- (3) *Estimate net soil N flux by measuring mineralization, nitrification, and plant uptake at TNEF.*

- (4) *Assess if soil IN pools increase throughout the growing season and are subsequently flushed to the stream during the dormant season.*
- (5) *Derive an lumped conceptual model that demonstrates forest response to declining atmospheric N deposition by predicting atmospheric and processed nitrate export from the watershed.*

It was expected that this watershed would be rapidly responsive to declining inputs and demonstrate similar proportional linear responses to that of other regional forests according to the predictions of the modified kinetic N saturation model (Eshleman et al. 2013). Furthermore I asserted that the N-status of this forest never progressed to higher stages of N-saturation because any excess  $\text{NO}_3\text{-N}$  accumulated during the growing season was flushed during the dormant months thus preventing the vegetative community from ever assimilating the excess IN.

## **Methods**

### *Site Location, Age, Past Demography, Land-Use History, and Soil*

The study was conducted within the 4 ha watershed of a tributary to Neff Run (TNEF, Fig. 1). The drainage ( $39^\circ 35' 47''$  N;  $78^\circ 54' 29''$  W) lies within the Appalachian Plateau of western Maryland. The watershed slopes steeply (averaging  $9.9^\circ$ ) from an elevation of 780 m down to 671 m on the northwest slope of Dan's Mountain near Frostburg, Maryland. The watershed is drained by an ephemeral stream, which is usually dry in late summer and early fall and during periods of drought (Negley and Eshleman 2006).

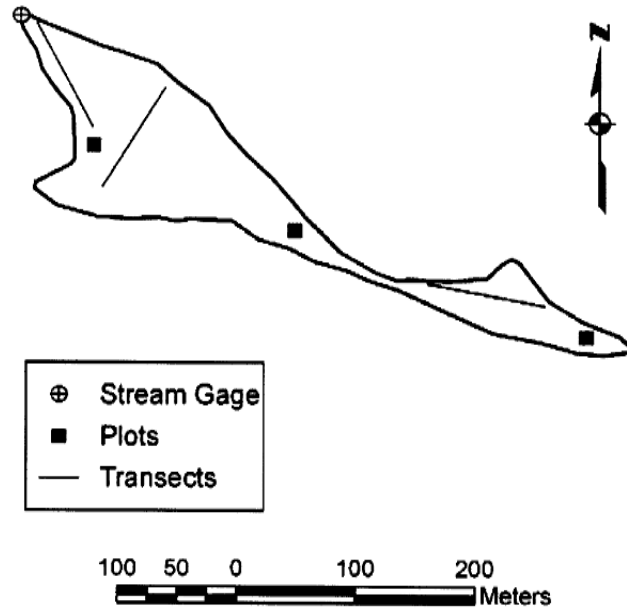


Fig. 1 Map of the TNEF watershed with the permanent sampling plots and permanent transects.

The TNEF watershed is completely forested, with the stand age ranging from 28-42 years (with some 80-100 year old individuals). The forest is within the humid continental climate zone with mild summers and relatively cold winters. Average monthly air temperatures range from  $-8.6^{\circ}\text{C}$  in January to  $26^{\circ}\text{C}$  in July. Annual precipitation averages 1132 mm and tends to be uniformly distributed throughout the year. Sugar maple (*Acer saccharum*) and black cherry (*Prunus serotina*) dominate (>60%) the above ground living biomass of  $108.6 \text{ Mg ha}^{-1}$  (Castro et al. 2007). The species distribution of the watershed includes: black cherry which is prevalent in the lower portions, northern red oak (*Quercus rubra*) more common on the upper portion, and sugar maples equally distributed throughout the watershed with larger individuals present in the middle of the watershed.

Previous historical records and field observations had indicated that the forest was commercially clearcut in the early 1980's with a number of older, smaller, and non-



merchantable stems left. About 15 years ago, TNEF was developmentally and structurally characterized as a young aggrading forest, with the young cohort accounting for 80% of the basal area of  $22 \text{ m}^2 \text{ ha}^{-1}$  and 95% of the  $5916 \text{ stems ha}^{-1}$  (Castro et al. 2007). Very few tree seedlings and herbaceous vegetation were present in the understory, in accordance with the effects of successive clearcuts of the forest (Meier et al. 1995; Elliott et al. 1997). The previous forest survey indicated the dominance of shade intolerant species (black birch, black cherry, sassafras, aspen, and black locust) present in the understory, providing further evidence of the clearcut.

The TNEF watershed is covered with soils of Cookport series (Stone and Matthews 1974). This class is a very stony loam weathered from acid sandstone (Castro et al. 2007). The Oe/Oa soil horizon has an average bulk density of  $0.032 \pm 0.015 \text{ g cm}^{-3}$ , an average pH of  $4.21 \pm 0.02$ , an average thickness of  $6.4 \pm 0.6 \text{ cm}$ , and a  $\text{Ca}^{+2}$  concentration of  $2.3 \pm 0.6 \text{ mg g}^{-1}$ . The upper 10 cm of mineral soil has an average bulk density of  $0.98 \pm 0.034 \text{ g cm}^{-3}$ , pH of  $3.97 \pm 0.03$ , a C:N ratio of 14, and total P concentration of  $1.2 \pm 0.8 \text{ mg g}^{-1}$ , and  $\text{Ca}^{2+}$  of  $2.2 \pm 0.8 \text{ mg g}^{-1}$  (Simmons et al. 2008).

#### *Stream water discharge and N fluxes*

Stream water discharge at TNEF has been continuously monitored since 1999 using a pre-fabricated, truncated Parshall flume with an attached stilling well housing a Unidata Model 6541 C digital water level recorder; instantaneous discharge can be readily computed from the known flume formula provided by the flume manufacturer (Freeflow, Inc.). Stream grab samples were collected on an event, weekly, or occasionally less frequent basis (i.e., during periods when the stream dried up) from October 2011 through September 2013 (two complete water years). One storm episode,

associated with the remnants of hurricane Sandy, was sampled intensively (12 samples day<sup>-1</sup>) with an ISCO 3700 sequential sampler from October 29 to October 31, 2013. Samples were filtered through 0.45µm filters within 24 h and frozen until analysis. Samples were analyzed for total dissolved N (TDN), NH<sub>4</sub>-N, NO<sub>2</sub>-N, and NO<sub>3</sub>-N using a Lachat +8000 series flow injection analyzer; dissolved organic N (DON) concentrations was computed by difference from the measured N species. Lachat colorometric procedures for NO<sub>3</sub>-N involve the quantified reduction of NO<sub>3</sub>-N to NO<sub>2</sub>-N by passage through a copperized cadmium column. After the reduction, the NO<sub>2</sub>-N was determined by diazotizing with sulfanilamide followed by coupling with N-(1-naphthyl)ethylenediamine dihydrochloride. Reagents for the NH<sub>4</sub>-N analysis include salicylate/citrate mixed solution and sodium dichloroisocyanurate solution. These reagents produce an alkaline hydrolysis reaction within the sample, which ultimately produces an indophenol-type compound following reactions with salicylate ions. TDN measurements utilized an alkaline persulfate/UV digestion to convert organic N to NO<sub>3</sub>-N prior to reacting the sample with the cadmium column and subsequent reduction to NO<sub>2</sub>-N.

Daily stream water N yields (kg ha<sup>-1</sup>) were computed as the product of a linearly-interpolated daily N concentration and the mean daily discharge using the WATFLOW model (Eshleman et al. 2008). These estimated daily values were summed to provide a complete set of monthly and annual N fluxes for the 2012 and 2013 water years—enabling direct comparison with comparable fluxes reported for the 2000-2004 water years by Castro et al. (2007).

Comparisons of estimated runoff and evapotranspiration with other predominantly forested watersheds in the region suggest that the true catchment area of TNEF is slightly greater (4 ha) than the value previously reported (3 ha) by Castro et al. (2007). For comparative purposes with recent data previously reported IN yields and runoff values have been adjusted in this paper assuming a 4 ha watershed area (note that reported flow-weighted concentrations are not affected by watershed area).

Precipitation was measured continuously in a clearing within two km of the study site using a Belfort Model 5-780 recording rain gauge fitted with a Belfort windshield. Weekly to bi-weekly bulk precipitation samples were collected at the Appalachian Lab in Frostburg, MD (moved from previous study site) and filtered through 0.45 $\mu$ m filters and were frozen until analysis. TDN, NH<sub>4</sub>-N, NO<sub>2</sub>-N, NO<sub>3</sub>-N and DON (by difference) were measured using the Lachat system. Weekly fluxes of wet deposition of N were estimated by calculating the weekly depth-weighted concentrations based on the daily precipitation records and the measurements of NH<sub>4</sub>-N, NO<sub>2</sub>-N, and NO<sub>3</sub>-N concentrations from the weekly bulk precipitation samples. Data from these sampling periods were then summed to estimate annual wet deposition values and depth-weighted concentrations.

#### *Isotopic Analysis*

Stream samples were also subjected to  $\delta^{15}\text{N}$ ,  $\delta^{18}\text{O}$ , and  $\delta^{17}\text{O}$  isotopic measurements on a modified Thermo GasBench II interfaced with an isotope ratio mass spectrometer as described by Casciotti *et al.* (2002) and Kaiser *et al.* (2007). Sample preparation for this analysis began with stream water NO<sub>3</sub>-N samples undergoing bacterial reduction using a strain of *Pseudomonas aureofaciens* to convert the dissolved NO<sub>3</sub>-N within the samples into nitrous oxide (N<sub>2</sub>O). No pre-concentration procedures

were required in this study since all stream samples had at least 200 nmol of NO<sub>3</sub>-N within 10 ml for isotope ratio mass spectrometry. Following sample preparation, the N<sub>2</sub>O is thermally converted to O<sub>2</sub> and N<sub>2</sub> at 730°C by reduction in a gold surface tube. After the decomposition, gases were further purified by gas chromatography (Finnigan Gas Bench II) before introduction into the isotope-ratio mass spectrometer (ThermoFisher Delta V+).

Three international reference materials were used to develop linearly interpolated calibration curves and serve as quality control standards between runs. USGS32 (KNO<sub>3</sub> salt) and USGS34 (nitric acid with δ<sup>18</sup>O depleted water) are used to calibrate δ<sup>15</sup>N values, whereas USGS34 and USGS35 (NO<sub>3</sub>-N ore deposits from Chile) are used to calibrate δ<sup>18</sup>O and δ<sup>17</sup>O values. USGS32 served as the quality control standard for δ<sup>18</sup>O and δ<sup>17</sup>O, whereas USGS35 offered δ<sup>15</sup>N check between runs. Atmospheric enrichment of streamwater NO<sub>3</sub>-N was calculated by a two-source mixing model (Michalski et al. 2004).

$$\%NO_3-N_{atm} = (\Delta O17_{sample} / \Delta O17_{atm}) * 100$$

(3)

A range of Δ<sup>17</sup>O<sub>atm</sub> (20 & 30) based on reported values was used to capture the maximum and minimum potential contributions of atmospheric NO<sub>3</sub>-N to the stream on an annual basis (Tsunogai et al. 2010). The Δ<sup>17</sup>O<sub>atm</sub> range is based on the seasonal variation in the oxygen enrichment anomaly in the troposphere, with higher values occurring during the winter months and lower enrichment occurring during the summer (Tsunogai et al. 2010). Calculated %NO<sub>3</sub>-N<sub>atm</sub> (eq.3) was applied to the measured total NO<sub>3</sub>-N concentration to determine processed and atmospheric NO<sub>3</sub>-N concentrations.

These separate NO<sub>3</sub>-N species were then used to generate separate yields using the WATFLOW model. Analytical isotopic precision (1σ) for the δ<sup>15</sup>N, δ<sup>18</sup>O, and ΔO17 procedures was 0.27 ‰, 0.57 ‰, and 0.13‰ respectively.

### *Soil Analyses*

Monthly *in situ* rates of net N mineralization, net nitrification, and standing pools of KCl-extractable NH<sub>4</sub>-N and NO<sub>3</sub>-N were measured within three permanent sampling plots during the 2012 growing season (May-November). Measurements were not taken during the dormant season since it has been reported that net IN production is negligible in the Southern Appalachians and about 10-15% of total production at Hubbard Brook (Knoepp and Swank 1998; Judd et al. 2007). Estimated standing NO<sub>3</sub>-N and NH<sub>4</sub>-N pools were not measured using the buried bag technique in November due to the major NO<sub>3</sub>-N flush that likely followed Hurricane Sandy in late October 2013. An absolute range of potential masses were reported based on the two scenarios of zero to complete IN immobilization. The range was based on the net mineralization and nitrification rates, and the initial October pool of IN within the two horizons. Standing pools of IN were resampled in May 2013 to assess changes in NH<sub>4</sub>-N and NO<sub>3</sub>-N pools following the 2013 dormant season. Soil samples were collected from three randomly selected subplots within each of the three permanent plots that had been established during the earlier study (Fig. 1). During each collection, a block of soil containing the entire forest floor and about 10 cm depth of mineral soil was removed from each subplot using a trenching shovel; the organic and mineral horizons were carefully separated on-site. A total of 18 samples (3 plots x 3 samples x 2 horizons) were taken at each collection. Approximately one half of each subsample was placed in a gas permeable polyethylene bag that was

placed back into the soil and allowed to incubate. The other half of each subsample was immediately returned to the laboratory where each sample was separately homogenized after dry sieving (2 mm mesh) and analyzed.

Approximately 10 g of each homogenized sample was preweighed, added to a 250 mL Erlenmeyer flask, into which 100 mL of 2M KCl solution was added to extract  $\text{NO}_3\text{-N}$  and  $\text{NH}_4\text{-N}$ . Solutions were mechanically shaken for one hour and filtered (0.45  $\mu\text{m}$ ) the following day; the filtered solutions were frozen until N analysis using the Lachat system. Other soil subsamples were used for a gravimetric determination of soil moisture following drying at 105° C. KCl-extractable N was computed in units of  $\text{kg g}^{-1}$  dry soil. Net N mineralization was calculated by taking the difference between the extractable  $\text{NO}_3\text{-N}$  and  $\text{NH}_4\text{-N}$  concentrations measured in *in situ* incubated samples and initial non-incubated samples per unit dry soil mass. Net nitrification was simply calculated by the difference between incubated and initial  $\text{NO}_3\text{-N}$  concentration per unit of dry mass of soil. These rates were scaled to  $\text{kg N ha}^{-1} \text{ mo}^{-1}$  and summed to produce annual rates ( $\text{kg ha}^{-1} \text{ yr}^{-1}$ ) using previously reported soil bulk density values for the plots (Simmons and Currie 2005). It should be noted that the field collection procedure deviated slightly from that of Castro et al. (2007), by taking a single large core at each sample site and splitting it into two portions, rather than using the paired core technique in the earlier study. This minor adjustment reduced variability and thus avoided the problem of dealing with negative rates acknowledged by Simmons et al. (2008).

Within-subjects repeated measures ANOVA analysis was utilized to evaluate changes in  $\text{NO}_3\text{-N}$ ,  $\text{NH}_4\text{-N}$  and IN ( $\text{NO}_3\text{-N} + \text{NH}_4\text{-N}$ ) standing pools ( $\text{kg ha}^{-1}$ ) from month to month in the 2012 dataset. Standing pool values of  $\text{NO}_3\text{-N}$ ,  $\text{NH}_4\text{-N}$  and IN were

log transformed in order to meet the distributional and homogeneity of variance assumptions of this analysis. Multiple models of repeated measures ANOVA were utilized in the exploration into the covariance/correlation structure in order to identify the most effective and parsimonious model. Once an adequate model was identified, the residuals from the model were assessed for normality using the Anderson-Darling test. Further post-hoc Tukey analysis was executed if warranted to determine specific pairwise differences.

Nitrogen standing pools, net nitrification rates, summer wet N deposition, and net mineralization rates were used to estimate vegetative uptake and leaching from the top 10 cm of soil using the following mass balance equation.

$$dIN/dt = \text{Net Mineralization} + \text{IN Deposition} - \text{Export} - \text{Plant Uptake} \quad (4)$$

Equation (4) can be expanded to determine net fluxes of NO<sub>3</sub>-N and NH<sub>4</sub>-N.

$$d \text{NO}_3\text{-N} / dt = \text{Net Nitrification} + \text{NO}_3\text{-N Deposition} - \text{Export (NO}_3\text{-N)} - \text{Plant Uptake (NO}_3\text{-N)} \quad (5)$$

$$d \text{NH}_4\text{-N} / dt = (\text{Net Mineralization} - \text{Net Nitrification}) + \text{NH}_4\text{-N Deposition} - \text{Export (NH}_4\text{-N)} - \text{Plant Uptake (NH}_4\text{-N)} \quad (6)$$

Plant uptake was estimated on a monthly basis from Eq. (5) and (6) since it cannot be readily measured. Leaching from the 10 cm of soil was assumed to be minimal during the growing season, enabling the elimination of the export term from the equations.

$$Plant\ Uptake\ (IN) = Net\ Mineralization\ (IN) + IN\ Deposition - dIN/dt$$

(7)

This approach allows for a simplified N budget for the Oe/Oa horizon and the top 10 cm of mineral soil during the growing season, using the above assumptions.

#### *Kinetic N-Saturation Model*

Lovett and Goodale (2011) proposed the kinetic N-saturation model to help understand the influence of atmospheric inputs on the outputs and storages of N in forested ecosystems:

$$D - V - S = Y + G$$

(8)

where  $D$  is N deposition,  $V$  is net incorporation of N into vegetation,  $S$  is net incorporation into soil,  $Y$  is the yield or export of N to surface waters, and  $G$  is the gaseous N loss (note, notation different from original paper). Eshleman et al. (2013) simplified this model further. If  $G$  is assumed to be small relative to  $Y$  and the  $V$  and  $S$  terms are combined ( $S + V = A$ ), then eq 7 can be simplified to:

$$Y = D - A$$

(9)

A simple solution to eq 9 can be obtained by making  $A$  a linear function of  $D$ :  $A=aD$  where the constant,  $a$  ( $0 \leq a \leq 1$ ), estimates the proportion of  $D$  that is taken up and stored in vegetation and soil. Substituting for  $A$  in eq 7:



$$Y = D - aD \text{ or } Y = D(1 - a)$$

(10)

This model predicts proportional decreases in forest NO<sub>3</sub>-N export to reductions in atmospheric N deposition with  $(1-a)$  serving as the proportionality constant. As stated previously in the introduction, this model was upheld for predicting NO<sub>3</sub>-N yield within predominantly forested watersheds (Eshleman et al. 2013). The present study further explores the D and  $(1-a)$  terms as part of an examination of the biogeochemical response of TNEF to declining atmospheric N deposition.

The model (eq 10) implicitly assumes that  $A \geq M$  where  $M$  is the net mineralization rate of IN since  $a$  is constrained between 0 and 1. If inputs of IN ( $I$ ) into the system are defined as:

$$M + D = I$$

(11)

and  $M = A$  if  $D = 0$ . This would lead to  $Y = 0$  according to eq 10. This situation has been observed for undisturbed temperate forest unimpacted by atmospheric N deposition (Hedin et al. 1995; Perakis et al. 2005; Pérez et al. 1998). If  $M$  is relatively constant over time (unaffected by deposition), while  $A$  is a linear function of D then  $D=I$ , since any nitrogen produced by mineralization will be immobilized by the system. Within the NO<sub>3</sub>-N pool itself, however the composition will be mixed between atmospheric and processed NO<sub>3</sub>-N. This leads to the yield and the net accumulation of atmospheric and processed NO<sub>3</sub>-N being determined by the proportion of the inputs.

$$M/I=P_p \text{ and } D/I=P_a$$

(12)

$$P_p I + P_a I = I$$

(13)

$P_a$  and  $P_p$  are the proportions that mineralization and deposition add to the net input of nitrogen outside of the scenario of  $M = A$  if  $D = 0$ . To solve for  $A$  of atmospheric ( $A_a$ ) and processed ( $A_p$ )  $\text{NO}_3\text{-N}$ :

$$A = A_T = A_p + A_a \rightarrow (P_p * A_T) + (P_a * A_T) = A_T$$

(14)

Substituting the derivations from eq 14 to eq 10:

$$Y_T = D - ((P_p A_T) + (P_a A_T))$$

(15)

And replacing  $A_T$  with  $aD$ :

$$Y_T = D - ((P_p aD) + (P_a aD))$$

(16)

Similar procedures will be carried out for determination of the atmospheric and processed  $\text{NO}_3\text{-N}$  yields.

$$Y = Y_T = Y_p + Y_a \rightarrow (P_p Y_T) + (P_a Y_T) = Y_T$$

(17)

In order to determine the atmospheric and processed  $\text{NO}_3\text{-N}$  yields, one must apportion  $D$  (which equals  $I$ ) according to processed and atmospheric proportions. Thus to solve for the processed yield:

$$Y_p = (P_p D) - (P_p aD)$$

(18)

And atmospheric yield:

$$Y_a = (P_a D) - (P_a a D)$$

(19)

Combined

$$Y_T = ((P_p D) - ((P_p a D))) + ((P_a D) - (P_a a D))$$

(20)

The kinetic N saturation model can be tested directly with the field data. An important implication from this model is that the ratio between processed and atmospheric NO<sub>3</sub>-N yield will be equivalent to the ratio of the inputs from atmospheric and internal sources.

$$Y_a / Y_T = D / I \text{ and } Y_p / Y_T = M / I$$

(21)

The model (eq 20) will produce a linear response to declines in N-deposition, while generating nonlinear responses in the proportions of atmospheric and processed NO<sub>3</sub>-N exported from the catchment. It effectively links atmospheric, soil, vegetative, and stream components by having these compartments interact via a dynamic IN pool within the soil matrix. This model solely models NO<sub>3</sub>-N yield since it is the predominant IN species yielded in this catchment and for forest regionally (Castro et al. 2007; Morgan and Kline 2011).

The model was applied to the TNEF catchment on an annual (water year) basis similar to the application in Eshleman et al. (2013) and an alternate model that incorporates the previous year's deposition to predict NO<sub>3</sub>-N yield for a particular year. The first model relied on estimated parameters *a*, *M*, and *D*. Based on previously observed export rates for TNEF, it is assumed the forest has very low retentive capacity

( $a = 0.10$ ).  $M$  is assumed constant over time, and a mineralization value of  $70 \text{ kg ha}^{-1} \text{ yr}^{-1}$  based on field data was utilized, while annual estimates for  $D$  relied on point extractions from National Atmospheric Deposition Program (NADP) GIS wet deposition maps with dry deposition estimates coming from the NADP Laurel Ridge site from 1986-2011 (NADP 2013). Wet deposition estimates for 2012-2013 relied on precipitation chemistry data generated from the current study with dry deposition estimates coming from the NADP Laurel Ridge site.

The alternate model predicted total, atmospheric, and processed  $\text{NO}_3\text{-N}$  yield relying on deposition and soil flux measurements to calculate the net accumulation rate  $A$  and  $P$  values for WY 2012-2013. This model tested the hypothesis that the majority of the  $\text{NO}_3\text{-N}$  exported in a given year is accumulated the previous growing season. At the end of the growing season (November 1<sup>st</sup>), soil  $\text{NO}_3\text{-N}$  pools were assumed to be completely flushed throughout the following dormant season, as such the pool served as the predictor for  $Y_t$  in Eq. 20.

In addition to model application, three different approaches were used to independently estimate the retention coefficient ( $a$ ) for the TNEF watershed.

- 1) The source contribution of total  $\text{NO}_3\text{-N}$  (microbial or atmospheric) was quantified within a spring baseflow sample, and by comparing the amount of atmospheric  $\text{NO}_3\text{-N}$  present in the stream and dividing it by the annual depth-weighted IN concentration within precipitation of the previous year a retention coefficient can be calculated. A range of dilution corrections ( $d$ ) was applied to the annual depth-weighted concentrations.

$$a = 1 - (\text{Stream } \text{NO}_3\text{-N}_{\text{atm}} / (\text{Atmospheric } \text{NO}_3\text{-N}_{\text{WY2012}} * d))$$

(22)

- 2) Relying on soil flux data generated from the buried bag techniques and atmospheric N deposition data,  $A$  (net accumulation) can be directly calculated. The difference between the net vegetative uptake ( $V$ , eq 7) and mineralization rate ( $M$ ) is the net accumulation ( $A$ ) of IN in a given year:

$$A = V - M$$

(23)

Following the net accumulation calculation, the retention coefficient will be the net accumulation divided by the total deposition for WY 2012.

$$A_{WY2012}/D_{WY2012} = a$$

(24)

- 3) The final approach used aggregated N budgets of the two study periods (2000-2004 & 2012-2013). This approach was carried out to smooth out hydrologic variability and establish if retention is constant overtime. The earlier study period was completely aggregated due to the extreme drought and subsequent flush that occurred from 2000-2004.

$$a = I - (Y_{2000-2004}) / D_{2000-2004}$$

and

$$a = I - (Y_{2012-2103}) / D_{2012-2013}$$

(25)

## Results

### *Atmospheric Deposition*

TNEF received 1024 and 1007 mm of precipitation during water years 2012 and 2013. This precipitation deposited 4.8 and 3.5 kg N ha<sup>-1</sup> yr<sup>-1</sup> of IN onto the catchment. Concentrations of NO<sub>3</sub>-N, NH<sub>4</sub>-N, and total IN in precipitation were lower than those reported by Castro et al. (2007) (table 1). Depth-weighted IN concentrations averaged 0.58 mg N L<sup>-1</sup> in the early 2000's and 0.41 mg N L<sup>-1</sup> in the 2012-2013 water years. NH<sub>4</sub>-N concentrations reported in this study were lower than those reported Castro et al. (2007). NO<sub>3</sub>-N concentrations in precipitation declined dramatically (0.30 mg N L<sup>-1</sup> to 0.20 mg N L<sup>-1</sup>). Our field measurements thus confirmed about a 29% reduction in atmospheric IN wet deposition at TNEF since the early 2000's, which is consistent with declines reported elsewhere. NADP/PRISM models demonstrated a 52% reduction since 1986, with declines beginning ~1997.

Table 1 Volume-weighted annual concentration of inorganic nitrogen in precipitation and annual wet deposition rates of IN at TNEF on a water year basis. Dry deposition estimates are on a calendar year basis.

Year	NH <sub>4</sub> -N Conc. (mg N L <sup>-1</sup> )	NO <sub>3</sub> -N Conc. (mg N L <sup>-1</sup> )	IN Wet Deposition (kg N ha <sup>-1</sup> yr <sup>-1</sup> )	Precipitation (mm)	Dry Deposition (kg N ha <sup>-1</sup> yr <sup>-1</sup> )*
2000	0.25	0.27	4.78	933	1.65
2001	0.40	0.47	9.00	1072	1.41
2002	0.36	0.33	6.29	944	1.43
2003	0.29	0.27	7.54	1399	1.28
2004	0.21	0.21	5.51	1341	1.10
2012	0.23	0.20	4.82	1024	0.86**
2013	0.15	0.20	3.48	1007	0.86**

\*Dry deposition rates are reported on a calendar year basis

\*\*Currently NADP has not reported dry deposition rates for 2012 and 2013. The average of the previous three years was taken and applied to 2012 and 2013 for reference.

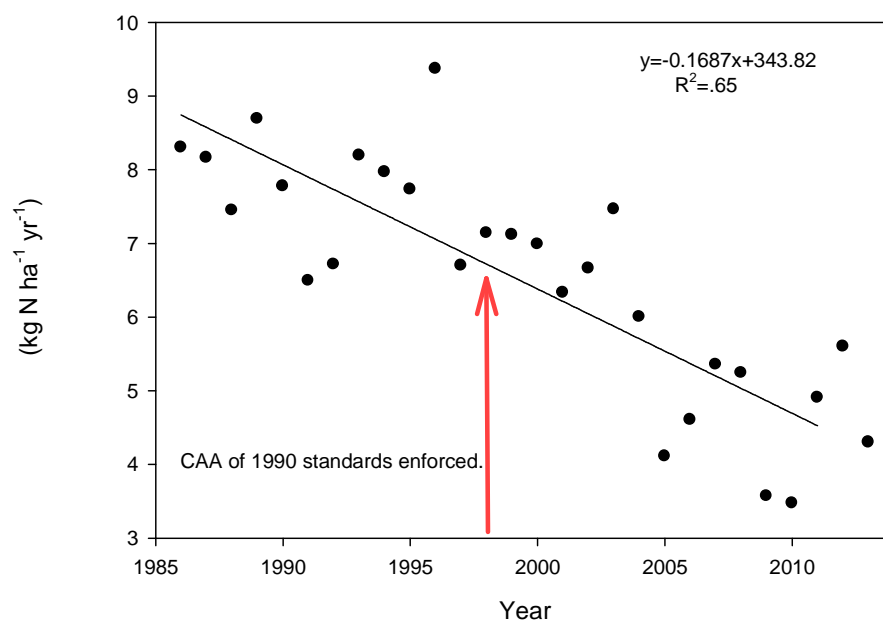


Fig. 2 Annual total IN atmospheric deposition (wet+dry) at TNEF from 1986-2011. Total deposition was calculated by combining modeled wet deposition rates from NADP/PRISM areal extracted values with reported dry deposition rates from a nearby NADP site at Laurel Ridge, PA. Linear regression was significant ( $P < 0.0001$ ).

### *Hydrology*

The period of study offered two distinct flow regimes in the 2012 and 2013 water years, even though annual precipitation was similar (1024 vs. 1007 mm). For water year 2012, sustained flow began at TNEF on October 2, 2011. Following a wet autumn, flows peaked in the month of January, but declined quickly following a relatively dry late winter and early spring period (fig. 3). There was very little snow accumulation with most precipitation falling as rain, which meant only a few minor snowmelt events occurred in 2012. The rapid spring decline was briefly offset during periods of intense and prolonged thunderstorm periods in early and late May following leaf-out (fig. 4). Flow at TNEF essentially ceased within a week after the 2012 derecho event in late June.

TNEF began flowing again on October 29, 2012 after receiving 115.5 mm of precipitation (rain to snow) from the remnants of Hurricane Sandy. November 2013 was extremely dry (8 mm of precipitation), but runoff was maintained by snowmelt from Sandy. Overall this pattern characterizes the water year 2013 winter and early spring flow regime, with multiple major snowmelts observed with some rain on snow events (fig. 4). Flows peaked in the late spring then quickly receded following leaf out (fig. 3). The difference in base flow values between May 2012 ( $0.0006 \text{ m}^3 \text{ s}^{-1}$ ) and May 2013 ( $0.0017 \text{ m}^3 \text{ s}^{-1}$ ) (fig. 4) emphasizes the drier conditions that were present in the late winter and early spring of water year 2012. Lower ET in water year 2013 combined with more snowmelt events in the winter and spring explain the higher annual runoff compared to water year 2012 (table 2).

Table 2 Annual flow-weighted average concentrations of  $\text{NO}_3\text{-N}$ , DON, IN, IN retention (IN annual yield/ Total IN Deposition), evapotranspiration (ET), and runoff for the TNEF watershed for 2000-2004 and 2012-2013 water years. Data for water years 2000-2004 from Castro et al. (2007) was adjusted to reflect use of 4 ha watershed area.

	$\text{NO}_3\text{-N}$ Conc. ( $\text{mg N L}^{-1}$ )	DON Conc. ( $\text{mg N L}^{-1}$ )	IN Yield ( $\text{kg N}$ $\text{ha}^{-1} \text{ yr}^{-1}$ )	IN Retention (%)	ET (m)	Runoff (m)
2000	2.12		3.33	48	0.78	0.16
2001	2.2		3.12	70	0.93	0.14
2002	3.09		3.99	48	0.81	0.13
2003	2.46		11.27	-28	0.94	0.46
2004	2.79		13.76	-108	0.85	0.49
2012	0.93	0.04	3.34	41	0.66	0.36
2013	0.95	0.06	5.41	-25	0.44	0.57



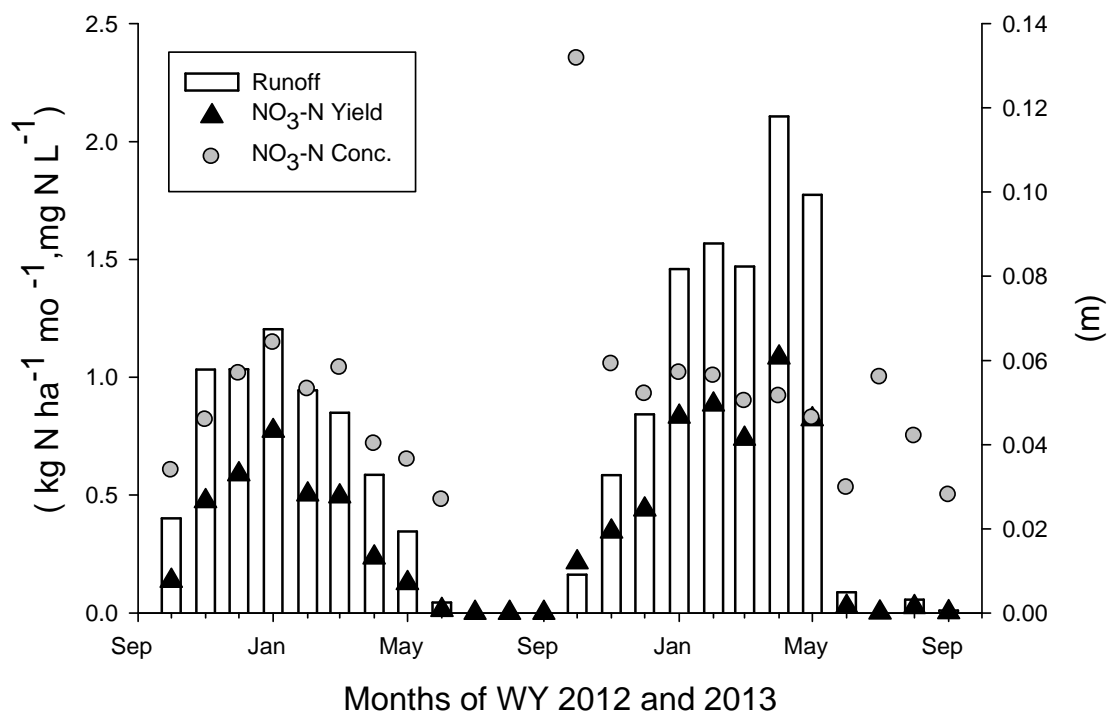


Fig. 3 Monthly flow-weighted concentrations and yields of NO<sub>3</sub>-N along with monthly runoff values for the 2012 and 2013 water year at TNEF.

#### *Streamwater N Yields and Concentrations*

NO<sub>3</sub>-N dominated stream water total nitrogen export from TNEF, accounting for 92 and 95% of streamwater N yield during water years 2012-2013. DON made up the second largest proportion of N yield at 7% and 4%, while NH<sub>4</sub>-N and NO<sub>2</sub>-N made up a small fraction at less than one percent. DON did not demonstrate any seasonal trends in export other than possible elevated concentrations in the summer and early fall. A distinct seasonality of monthly flow-weighted NO<sub>3</sub>-N concentrations was observed in water year 2012 (fig. 3), but no seasonality was observed in water year 2013, possibly due to the major NO<sub>3</sub>-N flush from hurricane Sandy following a three month flowless period (fig. 4). During the Sandy episodic sampling from October 29-31, 2012, a peak NO<sub>3</sub>-N concentration of 2.84 mg N L<sup>-1</sup> was observed just before peak runoff (fig. 5). Over the

three day sampling period,  $0.24 \text{ kg ha}^{-1}$  was flushed from the watershed, representing 4% of the total  $\text{NO}_3\text{-N}$  export for the year.

Annual  $\text{NO}_3\text{-N}$  yields from TNEF were  $3.34$  and  $5.41 \text{ kg ha}^{-1} \text{ yr}^{-1}$  for water year 2012 and 2013; both years produced similar flow-weighted concentrations ( $\sim 0.94 \text{ mg N L}^{-1}$ ). TNEF displayed inconsistent IN retention behavior during the two year study, functioning as a net sink of IN in 2012 (retaining  $2.3 \text{ kg ha}^{-1} \text{ yr}^{-1}$ ) and as a net source in 2013 (yielding  $1.07 \text{ kg ha}^{-1} \text{ yr}^{-1}$ ). Similar variable source and sink behavior was exhibited at TNEF in the early part of the 2000's (table 2). Annual flow-weighted average  $\text{NO}_3\text{-N}$  concentrations differed between the two study periods ( $2.57 \text{ mg N L}^{-1}$  in the early 2000's and  $0.94 \text{ mg N L}^{-1}$  for 2012-2013).

#### *Stable Isotope Analysis*

Atmospheric  $\text{NO}_3\text{-N}$  was detected in all but eight of the 72 stream samples analyzed from this study. The highest concentrations of atmospheric  $\text{NO}_3\text{-N}$  at TNEF were detected during major snow melts and rainstorm events where the initial baseflow was very low (fig. 4, fig. A1 in Appendix). Several of the elevated atmospheric  $\text{NO}_3\text{-N}$  concentrations were observed on the rising limbs of flood peaks. High concentrations of atmospheric  $\text{NO}_3\text{-N}$  within the stream samples are relatively short lived, with background concentrations returning within a matter of hours. The highest observed atmospheric concentration occurred on June 29, 2012 during a derecho event where the stream at TNEF had been dry for about two weeks prior to the event. Two grab samples collected at 22:00 and 22:30 showed atmospheric concentrations of  $\text{NO}_3\text{-N}$  at  $0.39$  and  $0.34 \text{ mg N L}^{-1}$  and processed  $\text{NO}_3\text{-N}$  concentrations of  $0.24 \text{ mg N L}^{-1}$  and  $0.97 \text{ mg N L}^{-1}$ .

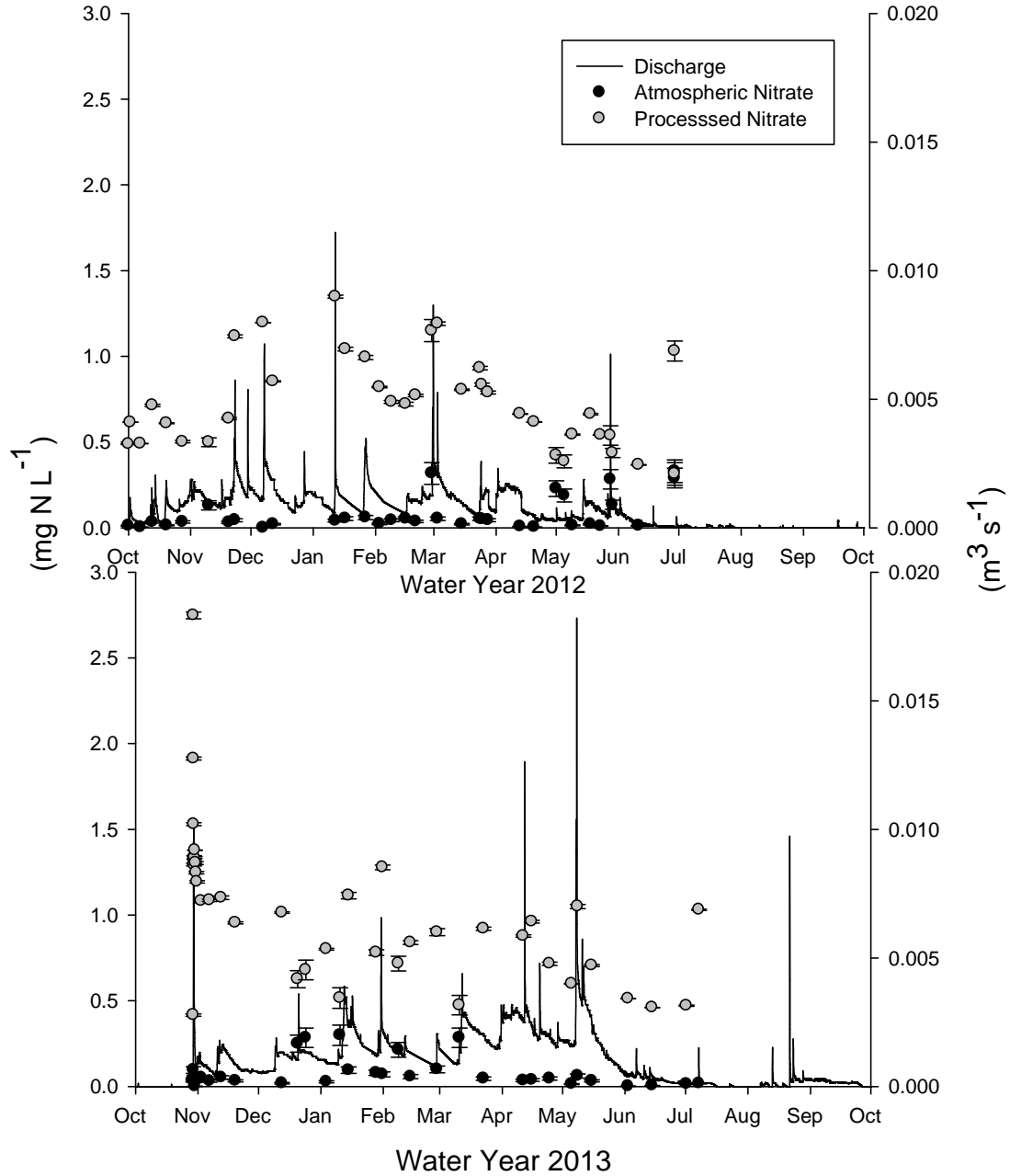


Fig. 4 Atmospheric and processed  $\text{NO}_3\text{-N}$  concentrations, error bars represent maximum and minimum range of atmospheric and processed concentrations. Instantaneous discharge values (15-minute data) are also shown.

Further isotopic analysis of the Sandy episode revealed that peak atmospheric  $\text{NO}_3\text{-N}$  concentration ( $0.12 \text{ mg N L}^{-1}$ ) had occurred when the proportion of new water

contribution was highest (just prior to the flood peak) to the stream (fig. 5, fig. A1). Overall atmospheric  $\text{NO}_3\text{-N}$  contributed little to the total  $\text{NO}_3\text{-N}$  yield for the event with processed  $\text{NO}_3\text{-N}$  making up over 99% of the export. The  $\Delta\text{O}17_{\text{atm}}$  signal was most likely dampened by the large amounts of processed  $\text{NO}_3\text{-N}$  built up within the soil in the summer of 2012 (fig. 8) and relatively low  $\text{NO}_3\text{-N}$  concentrations in the precipitation ( $0.01\text{-}0.10 \text{ mg N L}^{-1}$ ). The flush of  $\text{NO}_3\text{-N}$  from hurricane Sandy generated the highest monthly flow-weighted concentrations of processed  $\text{NO}_3\text{-N}$  in the fall for water year 2013, with apparent dilution occurring during the spring runoff (fig. 6).

Besides quick flow contributions of atmospheric  $\text{NO}_3\text{-N}$ , another pathway may involve a sudden upward shift in baseflow which is subsequently maintained constant by steady rains. In reference to December of water year 2013 (fig. 4, fig. A1), the initial December stream water collection was sampled two days after the dramatic rise in baseflow. The atmospheric  $\text{NO}_3\text{-N}$  concentration within the sample, following an extremely dry November (12.5mm of precipitation), was just  $0.02 \text{ mg N L}$ . Baseflow samples collected on 12/20 and 12/24 revealed surprisingly high atmospheric  $\text{NO}_3\text{-N}$  concentrations at  $.29$  and  $.34 \text{ mg N L}^{-1}$  within streams. The high concentrations must be attributed to rapid recharge and discharge of shallow groundwater that had been enriched with atmospheric  $\text{NO}_3\text{-N}$  during a period of low N processing and high atmospheric  $\text{NO}_3\text{-N}$  loading. Of the 119 mm of precipitation that fell over the three week period on the catchment revealed similarly elevated concentrations of  $\text{NO}_3\text{-N}$  at  $0.36 \text{ mg N L}^{-1}$ . Another period where steady precipitation maintained a relatively constant baseflow and elevated atmospheric  $\text{NO}_3\text{-N}$  in the stream was in May of water year 2012 (fig. 4, fig. A1).

Annual average flow-weighted concentrations of atmospheric  $\text{NO}_3\text{-N}$  were 0.04-0.06  $\text{mg N L}^{-1}$  for 2012 and 0.08-0.12  $\text{mg N L}^{-1}$  for 2013 (range for the atmospheric signals of  $\Delta\text{O}17_{\text{atm}} = 30$  and 20). Annual average flow-weighted concentrations of forest processed  $\text{NO}_3\text{-N}$  were 0.88-0.90  $\text{mg N L}^{-1}$  and 0.79-0.82  $\text{mg N L}^{-1}$  for 2012 and 2013, respectively. Processed  $\text{NO}_3\text{-N}$  thus dominates the TN yield with export values ranging from 3.18-3.26 and 4.44-4.65  $\text{kg ha}^{-1} \text{ yr}^{-1}$  for water years 2012 and 2013. Only 7-10% of the  $\text{NO}_3\text{-N}$  exported from TNEF was atmospheric  $\text{NO}_3\text{-N}$ .

A significant negative linear relationship was observed between processed  $\text{NO}_3\text{-N}$  concentration and the sample's  $\delta^{15}\text{N}$  signature (fig. 7). The lowest processed  $\text{NO}_3\text{-N}$  concentrations and highest  $\delta^{15}\text{N}$  signature were observed in the late spring, summer, and early fall months where baseflow runoff values are low and biotic processing is high indicating significant amounts of fractionation occurring from nitrification (fig. 8). Some of the lowest  $\delta^{15}\text{N}$  values were observed during the Sandy event where a large amount of processed  $\text{NO}_3\text{-N}$  was flushed from the system following the end of the growing season (fig. 5, fig. 7).

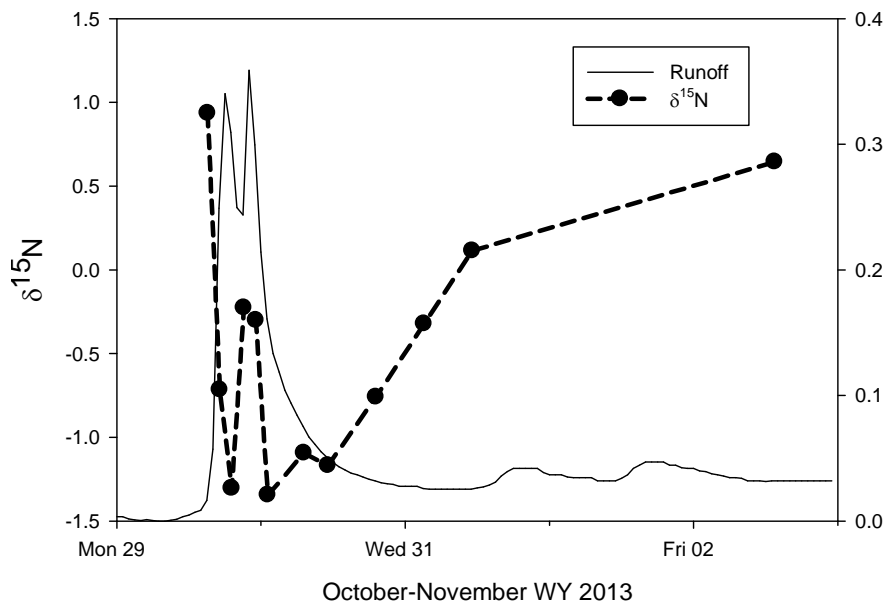
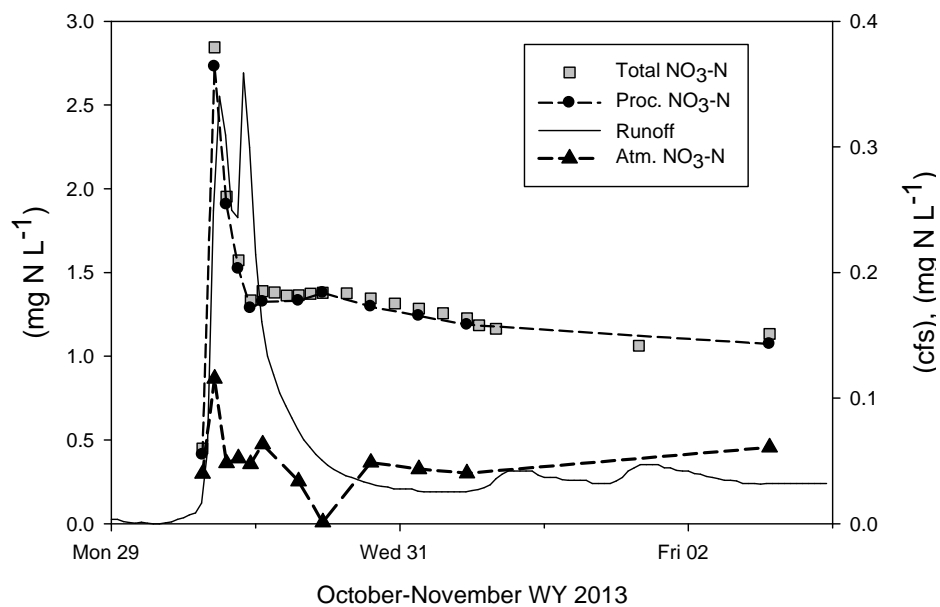


Fig. 5 Total (left y-axis), processed (left y-axis), and atmospheric NO<sub>3</sub>-N (right y-axis) concentrations following the hurricane Sandy episode in late October water year 2013. The bottom figure displays the NO<sub>3</sub>-N δ<sup>15</sup>N signature throughout the event.

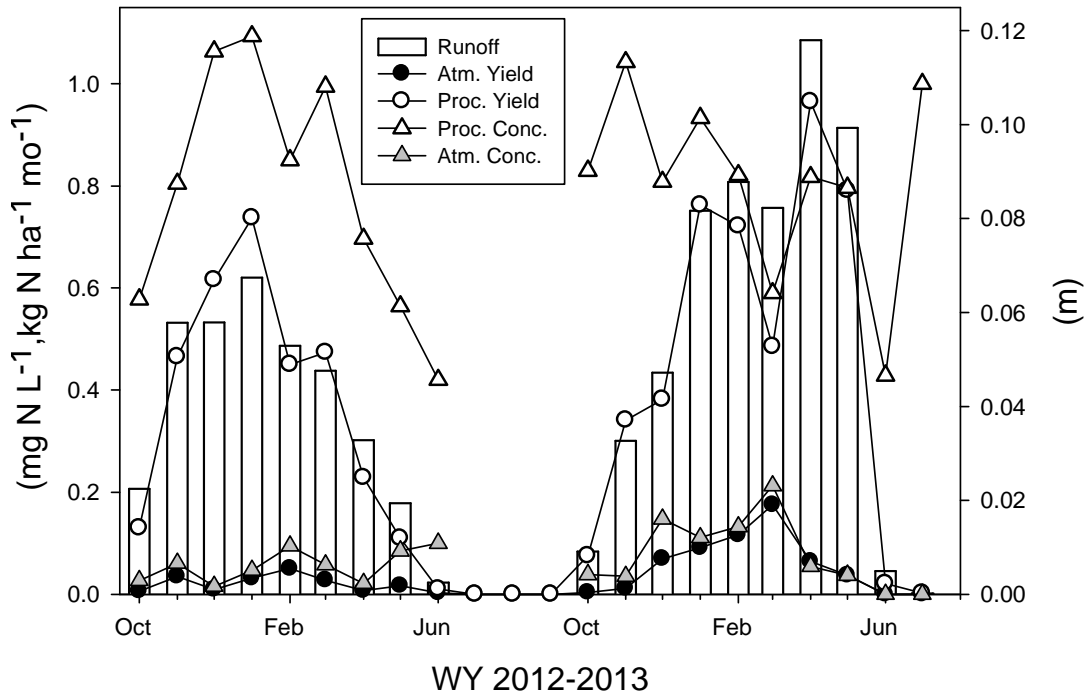


Fig. 6 Atmospheric and processed monthly flow-weighted average  $\text{NO}_3\text{-N}$  concentrations, monthly yields, and monthly runoff.

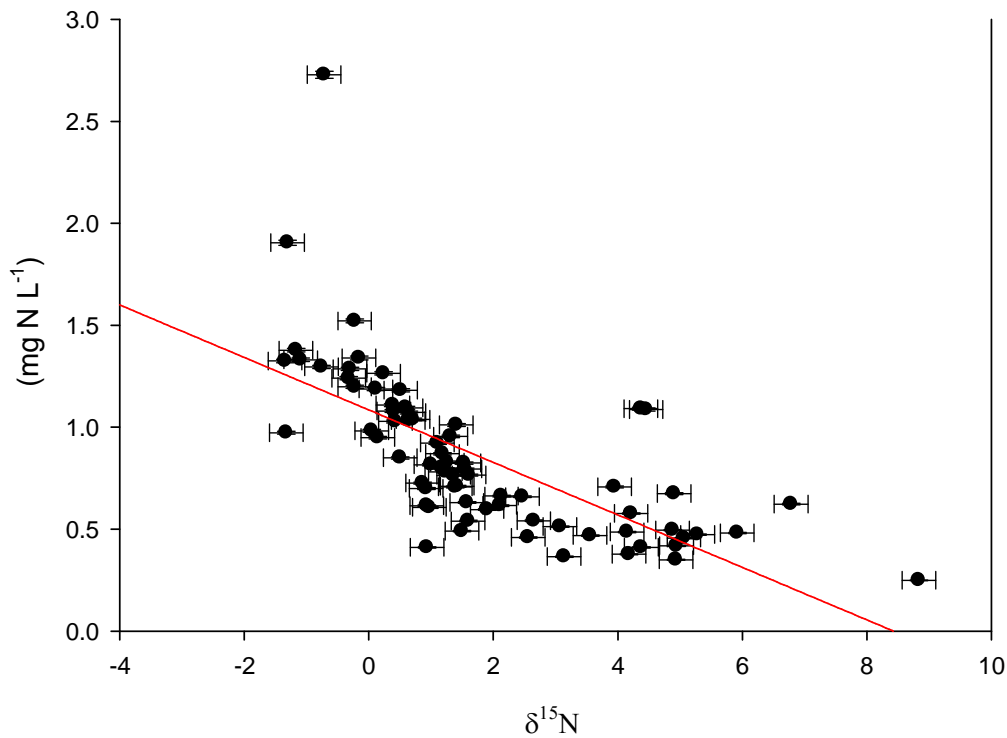


Fig. 7 Relationship between processed streamwater  $\text{NO}_3\text{-N}$  concentrations and their associated  $\delta^{15}\text{N}$  signal within  $\text{NO}_3\text{-N}$ . Linear regression was significant ( $P < 0.0001$ ).

Soil Net N Fluxes and Pools

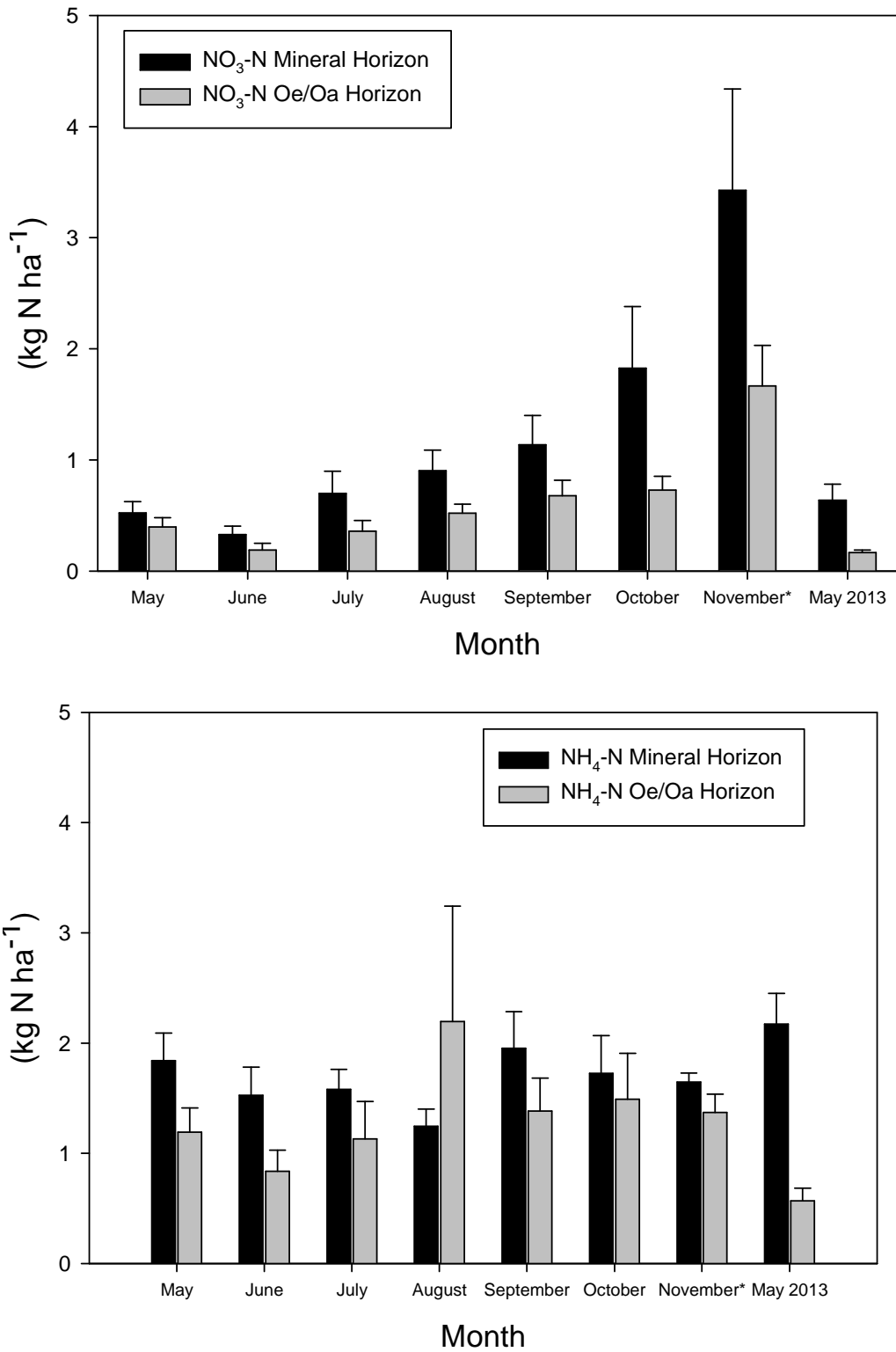


Fig. 8 Standing pools of inorganic nitrogen within the top 10 cm of soil during the 2012 growing season and May 2013 (following the dormant season flush) with standard error bars. \*Refer to Methods for details on the computation of November values.



Standing pools of IN increased from 3.95 ( $\pm 0.53$ ) to 5.77 ( $\pm 0.77$ ) kg ha<sup>-1</sup> in the Oe/Oa horizon and top 10 cm of mineral soil over the course of the 2012 growing season (fig. 9, ANOVA, p=0.042). This increase in IN, however, was not due to any significant shifts in the mass of NH<sub>4</sub>-N in the soil which remained nearly constant at 3.02 ( $\pm 0.15$ ) kg ha<sup>-1</sup> (ANOVA, p=0.90); rather, the increase was entirely due to an increase in NO<sub>3</sub>-N from 0.92 ( $\pm 0.16$ ) to 2.55 ( $\pm 0.59$ ) kg ha<sup>-1</sup> in the Oe/Oa horizon and top 10 cm of mineral soil (ANOVA, p=0.002, Fig. 8). Within the Oe/Oa horizon, the pool of NO<sub>3</sub>-N nearly doubled from 0.40 ( $\pm 0.08$ ) to 0.73 ( $\pm 0.12$ ) kg ha<sup>-1</sup>, while the mass of NH<sub>4</sub>-N lingered at 1.38 ( $\pm 0.22$ ) kg ha<sup>-1</sup>. The mineral layer's mass of NO<sub>3</sub>-N more than tripled from 0.52 ( $\pm 0.10$ ) to 1.83 ( $\pm 0.56$ ) kg ha<sup>-1</sup>, while NH<sub>4</sub>-N again remained relatively constant at 1.64 ( $\pm 0.07$ ) kg ha<sup>-1</sup> (Fig. 8). Overall there was a 1.63 kg ha<sup>-1</sup> gain of NO<sub>3</sub>-N from early May to October 1<sup>st</sup> which drove the observed increase in IN.

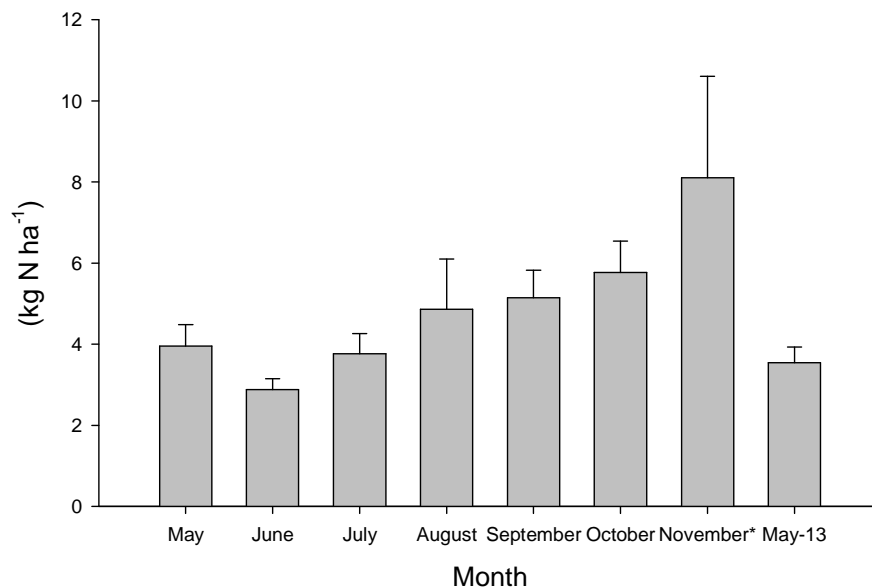


Fig. 9 Mean monthly pools of inorganic nitrogen within the top 10 cm of soil during the 2012 growing season and May 2013 following the dormant season flush.

Following the dormant season, the standing pools of  $\text{NO}_3\text{-N}$  in the Oe/Oa horizon and top 10 cm of mineral soil decreased from  $\sim 4.9(\pm 2.6, \text{ absolute range}) \text{ kg ha}^{-1}$  in November of 2012 (accurate measurement impossible due to major hurricane) to  $0.76(\pm 0.17) \text{ kg ha}^{-1}$  in May of 2013 (fig. 8).  $\text{NH}_4\text{-N}$  levels remained relatively constant at  $2.74(\pm 0.29) \text{ kg ha}^{-1}$  (fig. 8).  $\text{NH}_4\text{-N}$  pools within the Oe/Oa horizon for May 2013 were considerably lower compared to the May 2012 pool ( $0.57(\pm 0.11) \text{ kg ha}^{-1}$  to  $1.19(\pm 0.22) \text{ kg ha}^{-1}$ ); in addition  $\text{NO}_3\text{-N}$  was also lower at  $0.17(\pm 0.02) \text{ kg ha}^{-1}$  compared to the May 2012 pool of  $0.40(\pm 0.0832) \text{ kg ha}^{-1}$ . The IN pool decreased substantially throughout the dormant season within both horizons, and this loss is mainly attributed to the export of  $\text{NO}_3\text{-N}$ .

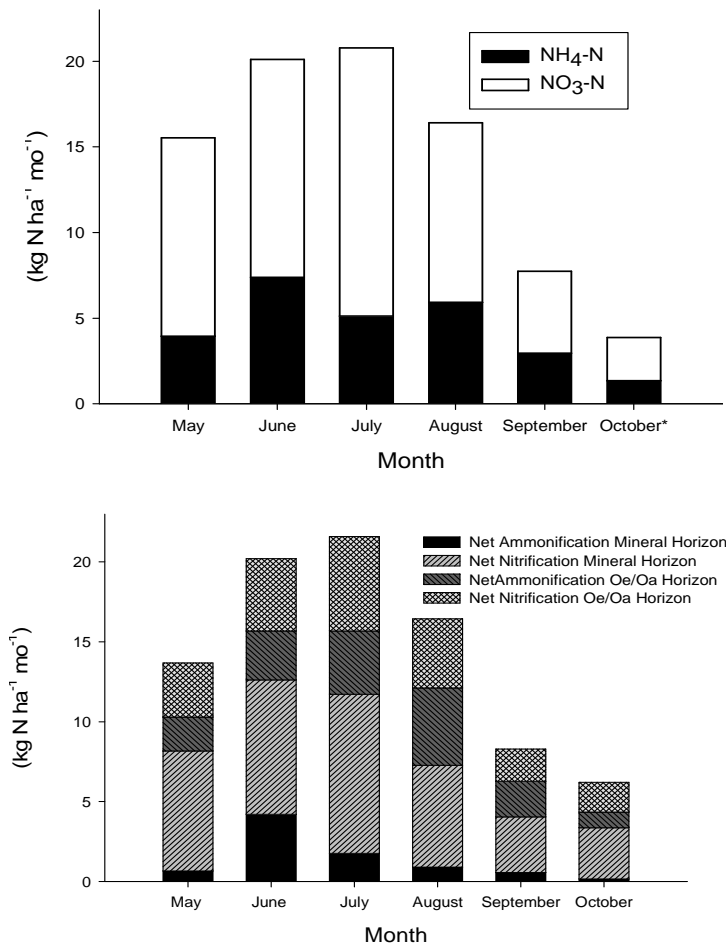


Fig. 10 Mean net vegetative IN uptake rates (top) within the Oe/Oa horizon and top 10 cm of mineral soil during the 2012 growing season. Net mineralization rates (bottom) are segmented into net  $\text{NH}_4\text{-N}$  and  $\text{NO}_3\text{-N}$  production rates within the Oe/Oa and lower mineral horizon.

The 2012 net mineralization rate for TNEF was  $86 \text{ kg ha}^{-1}\text{yr}^{-1}$  (May to October), whereas its net nitrification rate was  $61 \text{ kg ha}^{-1}\text{yr}^{-1}$  for the top 10 cm of mineral soil and Oe/Oa horizon (Fig. 10). The nitrification to mineralization ratio was 0.71 which translated into a lower net  $\text{NH}_4\text{-N}$  production rate of  $25 \text{ kg ha}^{-1}\text{yr}^{-1}$ . More specifically, the nitrification to mineralization ratio in the lower mineral layer was 0.82 for the total  $47 \text{ kg ha}^{-1}\text{yr}^{-1}$  of mineralized N, while in the Oe/Oa horizon it was 0.56 for the  $39 \text{ kg ha}^{-1}\text{yr}^{-1}$  of mineralized N (table 3). These higher ratios indicate that a high amount of mineralized  $\text{NH}_4\text{-N}$  was converted to  $\text{NO}_3\text{-N}$ , rather than being taken up by vegetation. Furthermore, the fluxes, as calculated using equation 1, suggest that mineralization rates were relatively balanced via plant uptake from May to September ( $80.21 \text{ kg ha}^{-1}\text{yr}^{-1}$  vs.  $80.58 \text{ kg ha}^{-1}\text{yr}^{-1}$ ). Net nitrification slightly exceeded net  $\text{NO}_3\text{-N}$  flux from the top 10 cm of mineral soil and Oe/Oa horizon ( $55.90 \text{ kg ha}^{-1}\text{yr}^{-1}$  to  $55.26 \text{ kg ha}^{-1}\text{yr}^{-1}$ ), while net  $\text{NH}_4\text{-N}$  flux actually exceeded net  $\text{NH}_4\text{-N}$  production ( $25.3 \text{ kg ha}^{-1}\text{yr}^{-1}$  to  $24.3 \text{ kg ha}^{-1}\text{yr}^{-1}$ ).

$\text{NH}_4\text{-N}$  pools remained relatively constant throughout the growing season due to high nitrification and uptake rates, while  $\text{NO}_3\text{-N}$  pools increased even in the face of high biotic demand. These elevated  $\text{NO}_3\text{-N}$  pools decreased significantly throughout the dormant season and they were thus unavailable to the vegetative community the following growing season.

Table 3. Rates of net N mineralization, net nitrification, and nitrification to mineralization ratios for water year 2012. Comparable data from 2000 and 2002 from Castro et al. (2007).

	Mineralization (kg ha <sup>-1</sup> yr <sup>-1</sup> )	Nitrification (kg ha <sup>-1</sup> yr <sup>-1</sup> )	NIT/MIN Ratio
2000*	46	38	0.83
2002*	76	73	0.96
2012-total	86	61	0.71
2012-Oe/Oa	39	22	0.56
2012-Min	47	39	0.82

\*2000 and 2002 mineralization and nitrification rates have been adjusted assuming a 4 ha watershed area.

### *Kinetic N-saturation Model*

Annual total NO<sub>3</sub>-N yield, as well as processed and atmospheric yield from TNEF was predicted from a range of atmospheric N deposition values (fig. 11). The model displays forest yield responding linearly to changing atmospheric deposition, similar to the modified kinetic N saturation model (Eshleman et al. 2013). The total NO<sub>3</sub>-N yield is the sum of two non-linear responses of atmospheric and processed yields (eq 18 &19). At current range of atmospheric N deposition (4-11 kg ha<sup>-1</sup> yr<sup>-1</sup>), atmospheric NO<sub>3</sub>-N yield in TNEF is small and makes up a small fraction of total NO<sub>3</sub>-N yield (5-10%). This small fraction is due to the fact that atmospheric N deposition only makes up a small proportion of total IN inputs into the system. These small N subsidies, however, substantially increase processed NO<sub>3</sub>-N yield within the stream of TNEF since the forest has a low retention factor of  $a=0.1$  (Fig. 11).

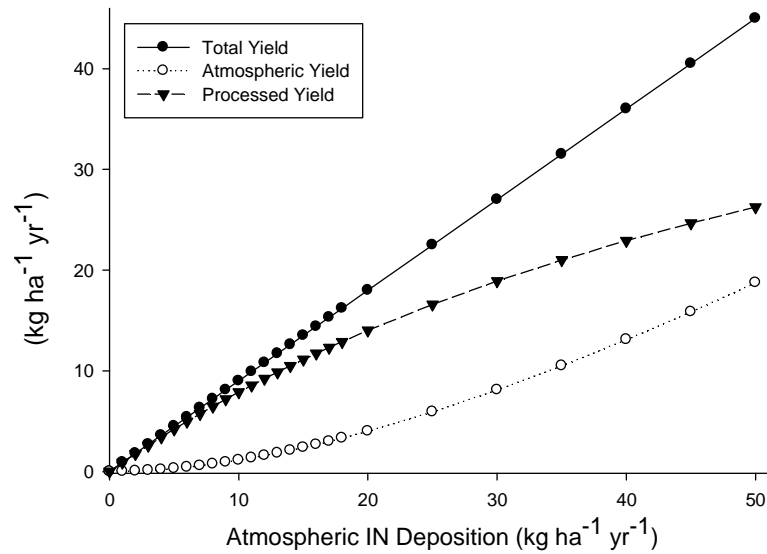


Fig. 11 Theoretical yield of total, atmospheric, and processed  $\text{NO}_3\text{-N}$  yield based on estimated parameters for TNEF ( $a=0.1$  and  $M=70 \text{ kg ha}^{-1} \text{ yr}^{-1}$ ). Processed, atmospheric, and total yield determined by eq 18-20.

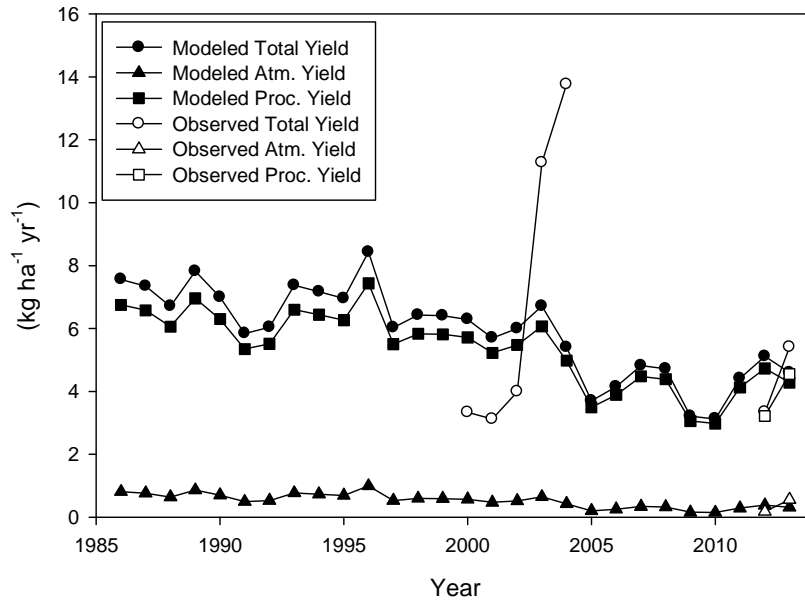


Figure 12 Modeled (eq. 20) and measured yields of total, atmospheric, and processed  $\text{NO}_3\text{-N}$  from TNEF. Estimated model parameters,  $a=0.1$  and  $M=70 \text{ kg ha}^{-1} \text{ yr}^{-1}$ .

The predicted annual processed, atmospheric, and total  $\text{NO}_3\text{-N}$  yields illustrate interesting temporal patterns that included two intensive study periods where yield was

measured (fig. 12). The model shows that total, atmospheric, and processed  $\text{NO}_3\text{-N}$  yields began to decline ~1997. The bulk of the decline in total yield is mostly attributed to decreases in processed  $\text{NO}_3\text{-N}$  yield, though both atmospheric and processed  $\text{NO}_3\text{-N}$  yield had equal proportional reductions of 45% since 1986. Inter-annual variability, however, was not well explained when compared with measured data from the two study periods. This disparity was not unexpected considering the offsetting of hydrologic transport processes that likely occurred during the prolonged drought which gripped the region from 1999-2002.

Though the model's reliability on an annual time scale is not high, when predicted annual yields are aggregated, they are much closer to the observed yield. For example total predicted yields at  $7.18 \text{ kg ha}^{-1} \text{ yr}^{-1}$  for the 2000-2004 period agreed with the observed yields at  $7.08 \text{ kg ha}^{-1} \text{ yr}^{-1}$ . A similar result was obtained for the 2012-2013 at  $4.28 \text{ kg ha}^{-1} \text{ yr}^{-1}$  for predicted total yields and  $4.37 \text{ kg ha}^{-1} \text{ yr}^{-1}$  for observed yields. These results highlight the efficacy of the model's utility to predict long-term mean forest response to changing atmospheric N deposition despite the lack of agreement at an annual timescale.

The annual model predicted atmospheric  $\text{NO}_3\text{-N}$  yields of  $0.32$  and  $0.22 \text{ kg ha}^{-1} \text{ yr}^{-1}$  for the 2012 and 2013 water years, respectively (fig. 12). These values are within a few tenths of a of the measured atmospheric  $\text{NO}_3\text{-N}$  yields of  $0.18$  and  $0.54 \text{ kg ha}^{-1} \text{ yr}^{-1}$  based on the use of  $\Delta^{17}\text{O}$  method and WATFLOW model. As in the case of the total  $\text{NO}_3\text{-N}$  yield, by aggregating the two water years, the modeled predictions and observation of atmospheric  $\text{NO}_3\text{-N}$  were closer at  $0.27$  vs.  $0.37 \text{ kg ha}^{-1} \text{ yr}^{-1}$ . Similarly by aggregating the two water years for processed  $\text{NO}_3\text{-N}$ , the modeled processed yield was

4.00 kg ha<sup>-1</sup> yr<sup>-1</sup> to 3.89 kg ha<sup>-1</sup> yr<sup>-1</sup> for measured. These results emphasize the importance of incorporating an understanding of hydrologic transport processes into the model, since the hydrology determines the timing of NO<sub>3</sub>-N delivery to streams.

A better understanding of the storage/release behavior could be better grasped by a comparison of the predicted NO<sub>3</sub>-N yields to the soil NO<sub>3</sub>-N pools. The predicted total, processed, and atmospheric NO<sub>3</sub>-N yield for water year 2012 is nearly identical to the processed and atmospheric yields of 2013. In light of this observation, the refinement relied on N-flux data from our water year 2012 soil, stream, and precipitation data, to attempt to predict water year 2013 NO<sub>3</sub>-N yield. The goal of this simple refinement was to demonstrate the impact of the previous water year on atmospheric and processed NO<sub>3</sub>-N yield during water year 2013. Due to the uncertainty of the mass of the NO<sub>3</sub>-N pool in early November, the estimation relied on an absolute range drawn from the estimated monthly net nitrification rates from October. The mass of the early October NO<sub>3</sub>-N pools was 2.55 kg ha<sup>-1</sup> and the net nitrification rate for the month was 5.08 kg ha<sup>-1</sup> mo<sup>-1</sup>. This led to an absolute range of 2.55-7.33 kg ha<sup>-1</sup> for the NO<sub>3</sub>-N pool in early November. The final NO<sub>3</sub>-N pool will ultimately determine the *A* and *Y*, so the absolute range of pool is reported in table 4.

Table 4. Results from the application of the alternate yield model (eq 16-18) relying solely on N-flux field measurements from water year 2012. Yield columns display predicted and observed (italics) values. Measured constants for *M*, *D*, *Pa*, and *Pp* are 86, 5.68, 0.06, and 0.94, respectively.

Soil NO <sub>3</sub> -N Pool	<i>A</i>	<i>Ya</i>	<i>Yp</i>	<i>Yt</i>
2.55	3.13	0.16 (0.45-0.64)	2.39 (4.44-4.65)	2.55 (5.41)
5.09	0.59	0.32(0.45-0.64)	4.77(4.44-4.65)	5.09(5.41)
7.33	-1.65	0.45(0.45-0.64)	6.88(4.44-4.65)	7.33(5.41)
<i>a=0.1*</i>	<i>A=aD</i>	0.32(0.45-0.64)	5.32(4.44-4.65)	5.64(5.41)

\**a=0.1\** term substitutes the measured soil and vegetative flux rates (*A*) with the estimated retention coefficient of TNEF (*A=aD*).

It is likely that the  $\text{NO}_3\text{-N}$  pool in early November 2013 was closest to  $5.09 \text{ kg ha}^{-1}$ . This intuition is confirmed based on the observed total yield for water year 2013. 6% of the November soil  $\text{NO}_3\text{-N}$  pool at the end of the growing season was made up of unprocessed atmospheric  $\text{NO}_3\text{-N}$ ; this value is within range of the reported proportions of atmospheric  $\text{NO}_3\text{-N}$  in soil, ground, and stream water reported elsewhere in other temperate forest. This led to a modeled atmospheric yield between  $.32 \text{ kg ha}^{-1} \text{ yr}^{-1}$  for water year 2013, which was below the measured values ( $.45\text{-}.64 \text{ kg ha}^{-1} \text{ yr}^{-1}$ ). The discrepancy can possibly be accounted by considering water year 2013 quick flow contributions where atmospheric  $\text{NO}_3\text{-N}$  bypasses the more circuitous baseflow route to the stream. Modeled processed  $\text{NO}_3\text{-N}$  export was  $4.77 \text{ kg ha}^{-1} \text{ yr}^{-1}$ , which was slightly elevated compared to measured yields of  $4.44\text{-}4.65 \text{ kg ha}^{-1} \text{ yr}^{-1}$ . Model uncertainty is mainly driven by estimates of the mass of the final  $\text{NO}_3\text{-N}$  pool at the end of the growing season, dormant season nitrification, and unaccounted direct contributions of atmospheric  $\text{NO}_3\text{-N}$  to the stream during water year 2013. Generally, modeling results highlight that the majority of  $\text{NO}_3\text{-N}$  (both atmospheric and processed) exported from the catchment in water year 2013 was accumulated during water year 2012 growing season (additional  $\text{NO}_3\text{-N}$  being added via quick flow during major storm and snow melt events).

This study explored alternative ways to determine retention coefficients in order to further explore the utility of this factor in assessing forest response to changing atmospheric N deposition. The spring sampling isotopic approach (eq. 22) revealed a retention coefficient of 8-29%, depending on the specific dilution factor used on the annual depth-weighted IN concentration of the previous water year (table A11). Data relying on soil measurements and atmospheric data was used to power equations 23 and



24 (summarized in table 4). The net accumulation term  $A=0.59 \text{ kg ha}^{-1} \text{ yr}^{-1}$  is divided by water year 2012 total deposition ( $5.6 \text{ kg ha}^{-1} \text{ yr}^{-1}$ ) which generates a retention coefficient of  $a= 0.11$ . The third and final approach, relying on long-term mass balances (eq. 24), generates 0.11 and 0.13 retention for the two study periods (2000-2004 and 2012-2013). Ultimately, all three independent approaches generated similar retention coefficients, relying on three distinct datasets (soil flux, isotopic, multi-annual mass balance).

## Discussion

As suggested by Castro et al. (2007), TNEF does not fit the expected N retention behavior of an aggrading forest with the catchment yielding extraordinarily high amounts of  $\text{NO}_3\text{-N}$ . The authors' characterization of TNEF as a stage III N-saturated forest, however, inadequately described the N status of this ecosystem and would fail to predict the dynamic response that TNEF has shown to reductions in atmospheric N deposition. The surprisingly high N yields at TNEF cannot be attributed to greater annual runoff or atmospheric N deposition. TNEF generated similar annual runoff values for water year 2012-2013 to nearby USGS gage stations for Georges Creek and Savage River near Barton. The watershed also received similar amounts of atmospheric N deposition, with our deposition measurements corresponding well with regional NADP observations at Laurel Ridge (PA83), Piney Reservoir (MD08), and Fernow (WV18). The NADP/PRISM wet deposition model demonstrated that TNEF had experienced a 52% drop in total N deposition since 1986 (if dry deposition is included based on data from Laurel Ridge) with the reductions beginning in 1997 (Fig. 2). This relative drop and

timing is consistent for other atmospheric IN deposition trends throughout the mid-Atlantic region.

Consistent with regional observations,  $\text{NO}_3\text{-N}$  yield from TNEF has decreased proportionally to reductions of total atmospheric N deposition over the past decade and produced similar retention coefficients to that of a nearby predominantly forested watershed (Eshleman et al. 2013). Though annual average flow-weighted  $\text{NO}_3\text{-N}$  concentrations at TNEF are still high relative to other forest in the region at  $\sim 0.95$  vs.  $0.05\text{-}0.40$   $\text{mg N L}^{-1}$  (Morgan and Kline 2011), the study revealed a 64% reduction in concentration since the early 2000's. This decline is similar to the 40-70% reductions reported by Eshleman et al. (2013) for other regional forest in a somewhat longer period of time. Such a rapid response to declining inputs of nitrogen was not expected due to the relatively small fraction that dry and wet deposition contribute to the plant available pool of IN within soils. These small N subsidies, however, kinetically saturated the vegetative and soil sink capacities of the ecosystem in turn fueling stream  $\text{NO}_3\text{-N}$  yield.

The study results suggests a very low N retention capacity ( $a= 0.10$ ) across a range of atmospheric N deposition ( $3\text{-}11$   $\text{kg ha}^{-1} \text{ yr}^{-1}$ ), yet reductions in atmospheric N deposition has driven a significant shift in the inter/intra-annual variation of N flux in the forest. TNEF in the early 2000's exhibited astoundingly high annual average flow-weighted concentrations of  $\text{NO}_3\text{-N}$  at  $2.57$   $\text{mg N L}^{-1}$ . In the most recent study period, only one monthly average flow-weighted concentration in our study period approached that concentration level of  $2.57$   $\text{mg N L}^{-1}$ ; that observation was made in October of 2013 at  $2.35$   $\text{mg N L}^{-1}$  during the hurricane Sandy event. During this three day event a substantial  $\text{NO}_3\text{-N}$  flushed occurred ( $0.24$   $\text{kg ha}^{-1}$  over three days), consistent with other flushes

associated with storm events (Inamdar et al. 2004). The initial study reported that  $\text{NO}_3\text{-N}$  flow-weighted average concentrations did not demonstrate strong seasonality throughout the year because consistently high concentrations were observed in the dormant and growing seasons. Our observations indicate apparent seasonality and a dampening of the dormant season concentration peaks in water year 2012(fig.4), consistent with that of other central Appalachian forests (Eshleman et al. 2013). Water year 2013 seasonality may have been offset by the flush of  $\text{NO}_3\text{-N}$  from subsurface quick flow during the Sandy event.

Remnants of hurricane Sandy precipitated a flush of  $\text{NO}_3\text{-N}$  from higher in the soil column. This meant that some of the  $\text{NO}_3\text{-N}$  produced in the summer had a shorter residence time and did not follow the usual dormant season hydrologic flow paths(Inamdar et al. 2004) . This translates into initially high  $\text{NO}_3\text{-N}$  concentrations in the fall, with relatively constant concentrations throughout the winter since a large sum of the excess  $\text{NO}_3\text{-N}$  never percolated down to be exported later in the in the dormant season. During the periods of likely quick flow,  $\delta^{15}\text{N}$  values were lowest and processed  $\text{NO}_3\text{-N}$  concentrations the highest (fig. 5.). This indicates that the source of  $\text{NO}_3\text{-N}$  where the quick flow passes through was highly concentrated and fractionated (Inamdar et al. 2004). Such conditions would exist in the top soil layers at TNEF where  $\text{NO}_3\text{-N}$  pools were observed to increase throughout the growing season (fig. 8).

Application of the  $\Delta\text{O}17$  tracer method was a powerful tool for exploring the mechanism that explains the intra-annual variability in streamwater  $\text{NO}_3\text{-N}$  concentrations and the impacts of atmospheric N subsidies on N-flux in forest. A substantial fraction of the exported total nitrogen (TN) over the study period was

atmospheric  $\text{NO}_3\text{-N}$  that had not undergone biotic processing (7-10%). This value is consistent with other  $\Delta\text{O}17$  studies that have reported 7-10% of total  $\text{NO}_3\text{-N}$  pools in streams, groundwater, and soil solution to be of atmospheric origin (Costa et al. 2011; Michalski et al. 2004; Tsunogai et al. 2010). Our analysis suggests that the proportion of atmospheric  $\text{NO}_3\text{-N}$  present within stream and soil water will simply be determined by the contribution of atmospheric N deposition to the total IN inputs into the system ( $I/D$ , eq 12). 84-88% of the TN had been  $\text{NO}_3\text{-N}$  that had undergone microbial processing, while DON made up the final 5% of export. These results indicate that atmospheric IN subsidies have a greater role in annual forest N biogeochemistry than once presumed (Costa et al. 2011).

The presence of atmospheric  $\text{NO}_3\text{-N}$  during baseflow conditions indicates that the  $\text{NO}_3\text{-N}$  pools within soils of TNEF are not completely exhausted. This is true despite the fact that net vegetative uptake rates are equivalent to net mineralization/nitrification rates ( $80.2$  to  $80.6 \text{ kg ha}^{-1} \text{ yr}^{-1}$ ) from May to September yet  $\text{NO}_3\text{-N}$  pools still increased by  $1.82 \text{ kg ha}^{-1}$  over the time period (fig. 8). This indicates that the net sink rates of  $\text{NO}_3\text{-N}$  are positive but are lower than the input rates (nitrification and deposition). This reveals that the nitrogen subsidies from wet atmospheric N deposition during the summer ( $1.79 \text{ kg ha}^{-1}$ ) and any atmospheric  $\text{NO}_3\text{-N}$  present at the beginning of the growing season saturated the abiotic and biotic kinetic N immobilization capacity of the soils and vegetation at TNEF.

The results from the isotopic analysis indicated that atmospheric contributions to stream water  $\text{NO}_3\text{-N}$  export follows two distinct paths. The first and less circuitous pathway involves the bypass of microbial processing via quick flow events either through

snowmelts or other major storm events (Campbell et al. 2006; Ohte et al. 2004). The determinant of the atmospheric contribution to stream water  $\text{NO}_3\text{-N}$  yield during these events will be a function of  $\text{NO}_3\text{-N}$  concentration in the precipitation and the amount of “new” water in the stream (Buda and DeWalle 2009). This study proposes a second pathway which involves a wave of atmospheric  $\text{NO}_3\text{-N}$  percolating through the soil column within the total  $\text{NO}_3\text{-N}$  pool and eventually being exported via baseflow. In order for the baseflow to display an atmospheric signal at any stage, the  $\text{NO}_3\text{-N}$  pool (processed +atmospheric) cannot be exhausted while traveling through the soil continuum to the stream. If that criterion is met then the mass of atmospheric  $\text{NO}_3\text{-N}$  will be function of the total  $\text{NO}_3\text{-N}$  pool and its starting proportion in the top layers of the soil and subsequent additions from mineralization and deposition.

Further evidence of the wave of  $\text{NO}_3\text{-N}$  being flushed through the soil continuum to the stream involves the negative relationship between processed  $\text{NO}_3\text{-N}$  and the  $\delta^{15}\text{N}$  signature. Lowest concentrations were observed in late spring and early summer, where catchment runoff contributing area is the lowest and soil depth is the deepest. High amounts of fractionation and uptake have occurred by the observation of enriched  $\delta^{15}\text{N}$  values and low proportions of atmospheric  $\text{NO}_3\text{-N}$  present in baseflow samples (fig. 6 & 7). This model deviates from the conventional view that plant uptake of nitrogen drops N export values in summer. Rather, this mechanism asserts that the flush of  $\text{NO}_3\text{-N}$  during the dormant season and subsequent immobilization at lower depths in the soil profile cause the observed declines. Groundwater and streamwater levels decrease as a result of increased ET thus causing soil depths more depleted in  $\text{NO}_3\text{-N}$  to contribute to stream flow.

More importantly, this mechanism will reconcile conflicting reports of summer  $\text{NO}_3\text{-N}$  peaks in the southern Appalachians and some Pennsylvania watersheds to the more conventional seasonal trends (Brookshire et al. 2011; Goodale et al. 2009). Forests that display summer  $\text{NO}_3\text{-N}$  peaks do not flush excess  $\text{NO}_3\text{-N}$  in the dormant season to the extent of more northerly temperate forest. This may be due to the fact that the soil  $\text{NO}_3\text{-N}$  pools within these forests do not significantly increase due to either high vegetative uptake or microbial immobilization capacity in soils. In this model when the soil wets up in the dormant season the concentration of  $\text{NO}_3\text{-N}$  in the stream is diluted rather than concentrated (Band et al. 2001). If this mechanism is correct, then temperate forests recovering from chronically high N-deposition may eventually show summer rather than winter/spring  $\text{NO}_3\text{-N}$  concentration peaks.

Overall the power of the isotopic  $\Delta\text{O}17$  conservative tracer of  $\text{NO}_3\text{-N}$  in streamwater was effective in demonstrating the impacts of atmospheric N deposition on temperate forest IN flux. Freed from fractionation biases inherent in the mixing analysis relying on  $\delta^{18}\text{O}$ , the method was able to demonstrate relatively low concentrations of atmospheric  $\text{NO}_3\text{-N}$  present in baseflow (Fang et al. 2012; Michalski et al. 2004). This observation provided evidence that IN deposition reaches the IN pool within soils and offsets the immobilization kinetics of forest as described in the model proposed in this paper.

The offsetting of the immobilization kinetics was explored through analysis of the intra-annual variability of N flux within the soils of TNEF and linking these observations to future N yield in streams. The 2013 *in situ* growing season net N mineralization rates for soils of TNEF was  $86 \text{ kg ha}^{-1} \text{ yr}^{-1}$  for the top 10 cm of soil. This rate is within the

range (30-200 kg ha<sup>-1</sup>yr<sup>-1</sup>) of annual N mineralization for temperate forest and is consistent with previously reported values for TNEF at 45 and 76 kg ha<sup>-1</sup>yr<sup>-1</sup> in 2000 and 2002 (Nadelhoffer and Raich 1992; Pastor et al. 1984; Nadelhoffer et al. 1984). Furthermore, the net mineralization and nitrification rate and nitrification to mineralization ratio of the mineral soil layer is consistent with other high NO<sub>3</sub>-N exporting forest in the region in the mid-1990's (Williard et al. 1997). Overall, the relative constancy in net nitrification and mineralization rates relative to past regional estimates provide confidence that a decline in net rates cannot explain the observed declining NO<sub>3</sub>-N trend. The decreased nitrification to mineralization ratio in 2012 (.71) compared to the 2000 and 2002 ratios (.82 and .96), may point to more efficient retention of mineralized NH<sub>4</sub>-N (Castro et al. 2007).

Only one published study has demonstrated possible rapid recovery of forest N-saturated soils following experimental reductions of IN inputs (Corre and Lamersdorf 2004). Our present data upholds their observations in a natural setting and further supports their speculation of tight microbial and abiotic coupling in reversing N-saturation by more efficient NH<sub>4</sub>-N retention in response to declines in atmospheric N deposition. This response can be integrated through a dynamic flushing mechanism which impedes N accumulation in the ecosystem (fig. 13). IN standing pools significantly increased throughout the growing season. This increase is driven by a substantial rise in the mass of NO<sub>3</sub>-N in the top 10 cm of soil, while the mass of NH<sub>4</sub>-N remained relatively constant. This steady state condition for NH<sub>4</sub>-N may be attributable to cation exchange and adsorption capacity of the soil (Carter and Gregorich 2007; Aber et al. 1989;

Vitousek et al. 1979). Any exchangeable  $\text{NH}_4\text{-N}$  released into soil solution is subsequently nitrified and vulnerable to leaching during the dormant season.

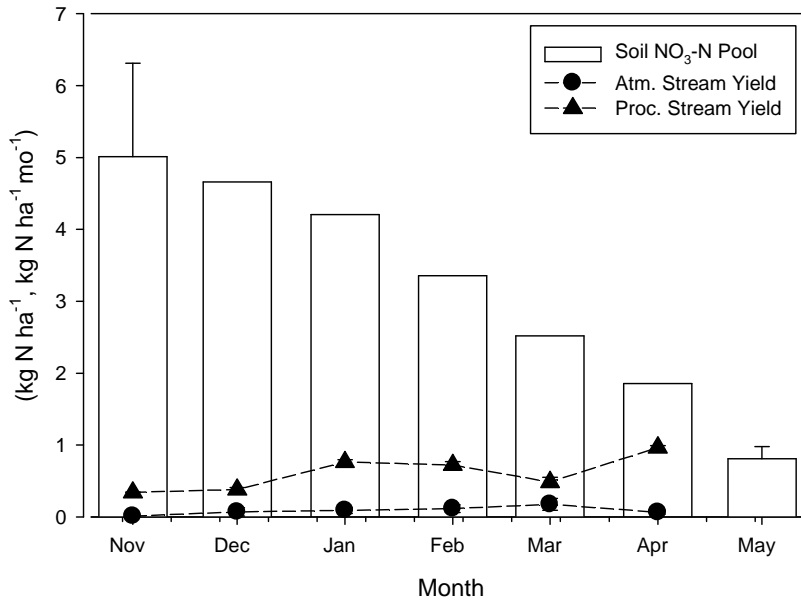


Figure 13. Decline in monthly soil  $\text{NO}_3\text{-N}$  pools throughout the course of the dormant season of water year 2013. Losses from the soil pools are attributed to the flush of  $\text{NO}_3\text{-N}$ , which is described by the monthly stream yields of atmospheric and processed  $\text{NO}_3\text{-N}$ .

This phenomenon seems to be supported by the high nitrification/mineralization ratio, higher net rates of  $\text{NO}_3\text{-N}$  flux to stream and vegetative compartments, and negligible amounts of  $\text{NH}_4\text{-N}$  being exported from the watershed. This behavior becomes most apparently displayed within the lower mineral layer where nitrification dominated mineralization and the observation of a significant build-up in  $\text{NO}_3\text{-N}$  from  $0.92(\pm 0.16)$  to  $2.55 (\pm 0.59) \text{ kg ha}^{-1}$  from May to October (Fig. 8). Since  $\text{NO}_3\text{-N}$  and net autotrophic nitrification is rarely observed in acidic temperate forest soils unimpacted by wet N-deposition (H. Persson et al. 1995; T. Persson and Wirén 1995; Pennington and Ellis 1993), it is seemingly apparent that any excess  $\text{NH}_4\text{-N}$  not abiotically or biotically immobilized is oxidized into  $\text{NO}_3\text{-N}$  thus making it highly probable the excess N will be



exported from the system during the dormant season. Such a flush was observed with  $\text{NO}_3\text{-N}$  pools dropping back down from  $\sim 4.9$  ( $\pm 2.6$  absolute range)  $\text{kg ha}^{-1}$  in November 2012 to  $0.76$  ( $\pm 0.17$ )  $\text{kg ha}^{-1}$  in May 2013 (fig. 13). This flush effectively prevents the vegetative community from acquiring this excess IN during optimal growing conditions, in turn offsetting the potential of the forest to substantially shift its N-status.

The relatively large amount of mineralized N being nitrified and the steady build-up of  $\text{NO}_3\text{-N}$  throughout the growing season lend support to the idea that hydrologic flushing of the soil contributes to a degree of N scarcity. Various flush types have been identified in a variety of systems and solutes (Boyer et al. 1997; Kaushal et al. 2008). It is well known that mineralization increases the pH in soils; it has also been demonstrated that some trees within forest that derive the majority of their N from  $\text{NO}_3\text{-N}$  tend to raise the pH of its surrounding rhizosphere, facilitating further nitrification (Persson et al. 1995). Even though the reduction of  $\text{NO}_3\text{-N}$  is considered to be more energetically costly for the plant, the alkalinizing effect on soils may help trees avoid  $\text{NH}_4\text{-N}$  toxicity by ensuring excess  $\text{NH}_4\text{-N}$  gets nitrified. In turn, more IN is still available to the trees but the assimilation of IN (via  $\text{NO}_3\text{-N}$ ) is rate limited by the plants ability to maintain its charge balance within cells (Imsande and Touraine 1994). Furthermore, a dormant season flush of  $\text{NO}_3\text{-N}$  essentially resets IN pools which ensures that the vegetative community lacks access to the excess IN for the following growing season. This mechanism could explain why some temperate ecosystems suffer from declining N-availability even in the face of chronic inputs of atmospheric N deposition (McLauchlan et al. 2007; McLauchlan et al. 2010).

During dry periods,  $\text{NO}_3\text{-N}$  pools may not get completely flushed, particularly during the winter months, and the soil N pools at the beginning of the growing season are much higher and would be expected to increase much more rapidly due to additional N excess during the growing season (Bechtold et al. 2003). These conditions may explain the extraordinarily high  $\text{NO}_3\text{-N}$  export values in 2003 and 2004 at  $12\text{-}14 \text{ kg ha}^{-1} \text{ yr}$  following three years of drought stress (Castro et al. 2007). It was predicted that  $\text{NO}_3\text{-N}$  pools would be raised to  $\sim 4.9(\pm 2.6 \text{ absolute range}) \text{ kg ha}^{-1}$  following estimates from the October IN additions from net nitrification and possible  $1\text{-}2 \text{ kg ha}^{-1}$  of IN immobilization by leaf litter (Piatek and Adams 2011). After considering microbial and abiotic immobilization pathways during the dormant season, one sees that this value is well within the range of potential  $\text{NO}_3\text{-N}$  export of  $5.4 \text{ kg ha}^{-1} \text{ yr}^{-1}$  for the following 2013 dormant season. Essentially the final  $\text{NO}_3\text{-N}$  pool will be  $Y$  in the modified kinetic N saturation model. The flushing mechanism presented within this section offers a possible parsimonious mechanism to explain declining  $\text{NO}_3\text{-N}$  export for forest throughout the east coast of the USA and unexpectedly high  $\text{NO}_3\text{-N}$  yields experienced at TNEF in the early 2000's. It is assumed that TNEF along with other forested watersheds will likely continue to respond to reductions in atmospheric deposition.

The importance of this flushing mechanism in preventing forest from attaining higher stages of N-saturation could not be developed without intensive short-term analysis of the intra-annual variability of stream and soil  $\text{NO}_3\text{-N}$  flux. These observations effectively linked the different ecosystem compartments of temperate forest and provided understanding into the primary drivers of short and long-term trends of N-flux in ecosystems. This analysis revealed the interactive effects amongst years in driving N-

yields and emphasizes that annual time series analysis is not necessarily appropriate for linking the effects of deposition on N flux. Applications of these insights were applied in a mechanistic model to address the influence of deposition at various time scales.

#### *Application of the Expanded Modified Kinetic N Saturation Model*

This paper, based on the stated observations, upholds Lovett and Goodale (2011) and Eshleman et al. (2013) utilization of the kinetic N saturation model in unifying our understanding of the N-biogeochemistry of forested systems. Rather than focusing on the temporal patterns of key N cycling indicators as in the dominant conceptual model of N saturation, the expanded kinetics model developed within this paper focuses on the mass balance of N. It effectively links atmospheric, soil, vegetative, and stream compartments by having these parts interact integratively via a dynamic IN pool dissolved in the soil continuum. This study explored these interactions through a simplified relationship, where the yield was a simple linear function of deposition ( $Y=aD$ ). Application of the annual model revealed an efficacy for maintaining long-term mass balances yet failure to capture the inter-annual variation. Further refining this relationship by inserting interactions amongst year, the model was adjusted to incorporate the storage/release behavior of NO<sub>3</sub>-N within TNEF in turn reconciling observed soil NO<sub>3</sub>-N pools with observed stream yields.

Since the soil NO<sub>3</sub>-N pool is not exhausted due to mineralization (86.44 kg ha<sup>-1</sup> yr<sup>-1</sup>) continuously and deposition (5.68 kg ha<sup>-1</sup> yr<sup>-1</sup>) episodically adding to the IN pool, it was predicted by the refined model that atmospheric and processed NO<sub>3</sub>-N yields will be proportional to the annual inputs. Deposition made up 6% of the inputs to the IN pool at TNEF for water year 2012, while mineralization contributed the remainder (table 4). This

led to a predicted flush of atmospheric and processed  $\text{NO}_3\text{-N}$  yield of 0.32 and 4.77  $\text{kg ha}^{-1} \text{yr}^{-1}$ , respectively, for water year 2013. These estimates were well within range of the measured 0.45-0.68 and 4.44-4.65  $\text{kg ha}^{-1} \text{yr}^{-1}$  of atmospheric and processed  $\text{NO}_3\text{-N}$  exported over the water year 2013 dormant season. Some disagreement between predicted and measured values can be attributed to possible greater direct contributions of atmospheric  $\text{NO}_3\text{-N}$  from snowmelt events during water year 2013 and uncertainty over the final  $\text{NO}_3\text{-N}$  pool in November (Goodale et al. 2009; Campbell et al. 2006). The application of the alternate model, parameterized with field data, confirms the overwhelming effect of the previous year's N-flux in determining the next year's  $\text{NO}_3\text{-N}$  export and how deposition directly impacts the kinetics of N immobilization in a watershed.

It is apparent from our varied application of the kinetic N saturation model that declines in nitrogen deposition have decreased the amount of atmospheric  $\text{NO}_3\text{-N}$  being directly contributed to the stream water  $\text{NO}_3\text{-N}$  yield and allows forest to be more efficient in retaining mineralized nitrogen by adding less substrate to the standing IN pool. Furthermore, through the model, one can generate consistent retention coefficients (eqs 22-25) that may bypass the need for long-term water quality records to evaluate the ability of a forest to retain atmospheric N deposition. These coefficients can be used to power the modified kinetic N saturation model and the expanded version presented in this paper to predict  $\text{NO}_3\text{-N}$  yield for forest in mixed land-use watersheds. Further identification of retention coefficients in a declared "stage-III N-saturated forest" suggests that community models could be used to explore the spatial variability of forest N yield. Another important insight from these calculated retention coefficients is that N

retention is not determined by historic deposition rates rather it is the site and regional specific drivers that determine the retention capacity of forest.

The accuracy generated by this parsimonious model illustrates two important concepts for future model development. The first is that hydrology governs the timing of the  $\text{NO}_3\text{-N}$  export, which causes interactions amongst years. The  $\text{NO}_3\text{-N}$  accumulated over the previous year is flushed during following dormant season (Castellano et al. 2013). During that flush direct atmospheric contributions vary from year to year depending on the precipitation type and magnitude of events. This issue is illustrated with the annual model being effective at maintaining long-term mass balances yet displaying greater inaccuracy at the annual time-step (fig. 12). The question then arises on why the behavior of the larger pre-dominantly forested watersheds ( $1.0 \text{ km}^2$ - $10,500 \text{ km}^2$ ) of the Eshleman et al. (2013) study were able to be explained through solely the annual model and TNEF needed the refinement. This may be due to the lack of reliable groundwater within the small, steeply sloped catchment of TNEF. Groundwater contributions of larger forested catchments may integrate the influence from the previous 2-3 years of deposition and hydrology. This longer residence time contributes to “smoothed” responses even in the face of extreme hydrologic conditions, such as the drought observed in the early 2000’s. This explanation highlights the need to further understand the hydrologic drivers of  $\text{NO}_3\text{-N}$  storage and release, and the role hydrology plays in maintaining mass balances.

The second important concept is that empirically derived retention coefficients proposed by Eshleman et al. (2013) and Grigal (2012) at the current range of atmospheric deposition, are real and have predictive prowess in projecting forest response to atmospheric N deposition. These linear relationships are produced by the summed non-

linear yield responses of processed and atmospheric  $\text{NO}_3\text{-N}$  yield, and suggest that the N-status of forests do not shift into higher states of N-saturations (fig 11). The model described in fig. 11, projects very little atmospheric  $\text{NO}_3\text{-N}$  yield at the lower end of deposition ( $0\text{-}15 \text{ kg ha}^{-1} \text{ yr}^{-1}$ ). The increased deposition however directly impacts the amount of processed  $\text{NO}_3\text{-N}$  yielded by adding to the available IN pools within soils thus straining the immobilization capacity of the forest (even though the net accumulation proportionally increases). The extent of this response will be dependent on the inherent sink capacity of the forest, which warrants future empirical investigations as more long-term records and approaches described in this paper become available. Overall the discovery of minimal amounts of atmospheric  $\text{NO}_3\text{-N}$  present in stream water or lack of direct annual correlation between deposition and stream  $\text{NO}_3\text{-N}$  yield should not be grounds to dismiss deposition as a significant driver of IN flux within forest.

This study has established that an “N-saturated forest” can respond rapidly to reductions in atmospheric N deposition (table 2, fig. 3), demonstrated significant export of atmospheric  $\text{NO}_3\text{-N}$  in storm and base flow sampling (fig. 4,5,& 6), and linked soil  $\text{NO}_3\text{-N}$  flushes with proceeding annual stream  $\text{NO}_3\text{-N}$  yield (fig. 8, table 4). The  $\text{NO}_3\text{-N}$  flush effectively links atmospheric, soil, vegetative, and stream compartments of the temperate forest ecosystem. In light of the conceptual framework of a  $\text{NO}_3\text{-N}$  flush, which is applicable to all temperate forest, led us to propose a lumped conceptual model building on the kinetic N saturation concept to demonstrate how forest can respond annually to changes in deposition. This conceptual model and mechanism should launch more effective synthesis of our understanding of N-flux in forest and offer insights into the development of sound policy decisions.

## Appendix

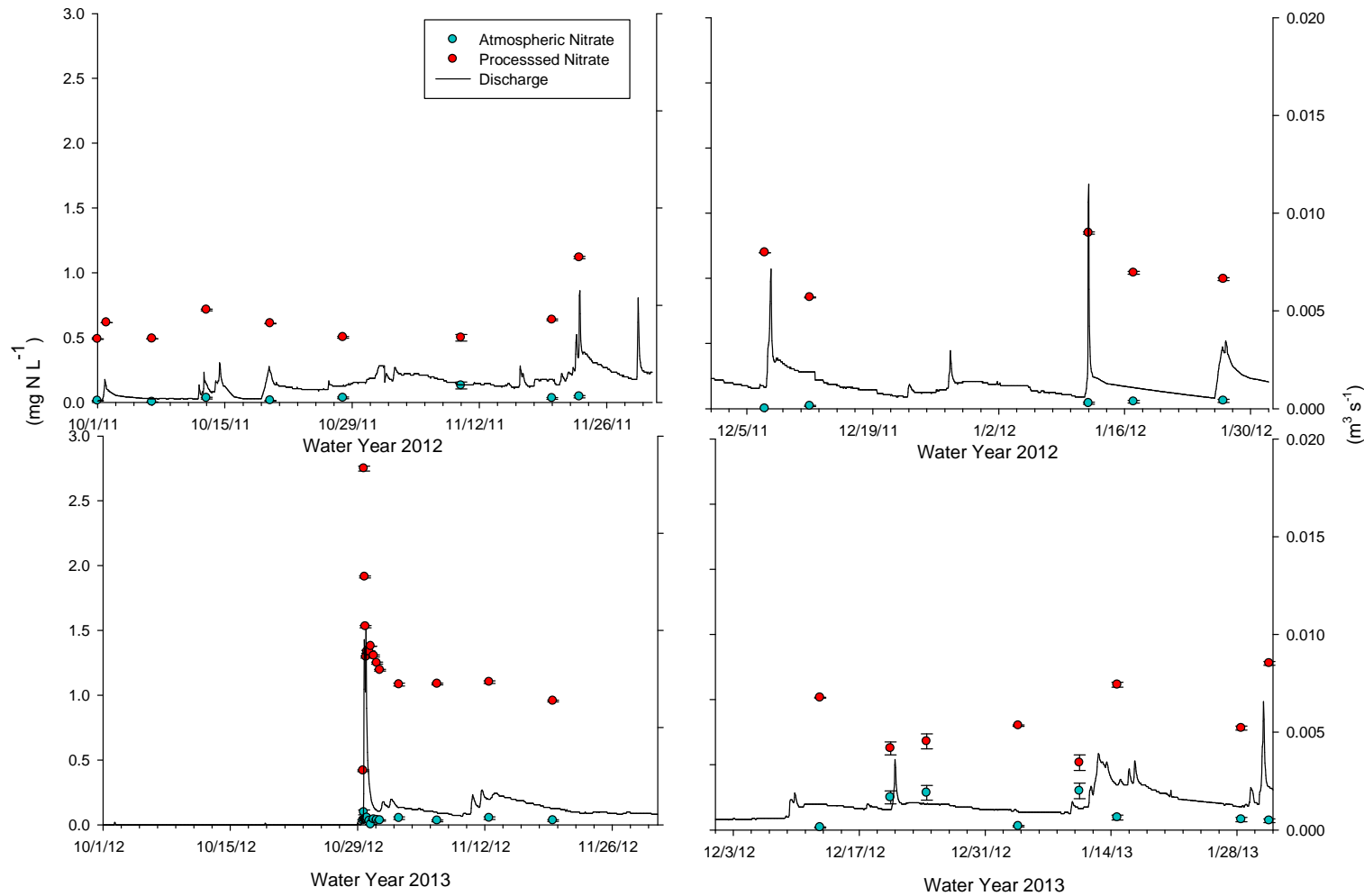
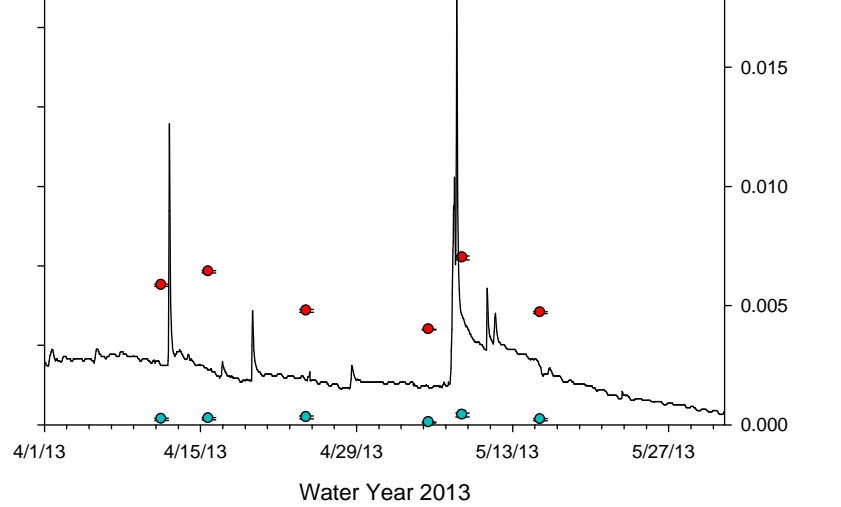
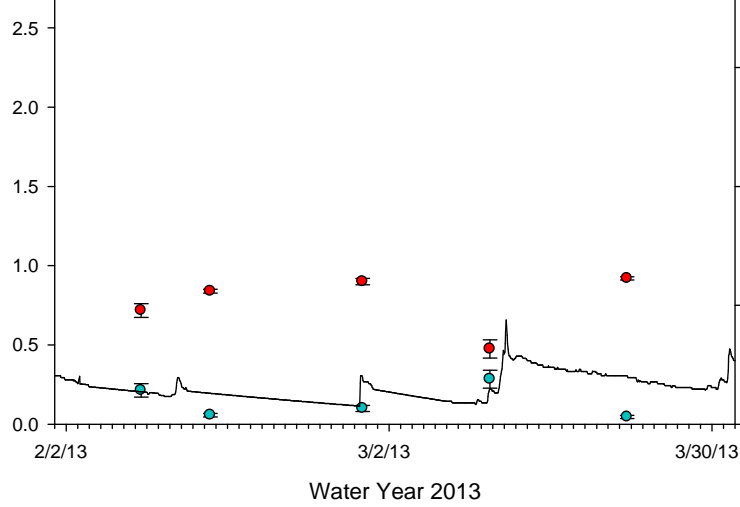
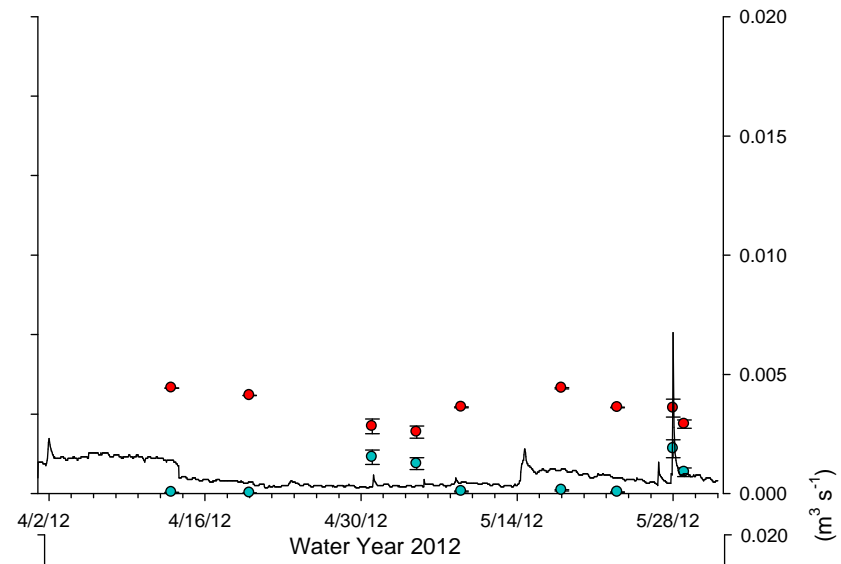
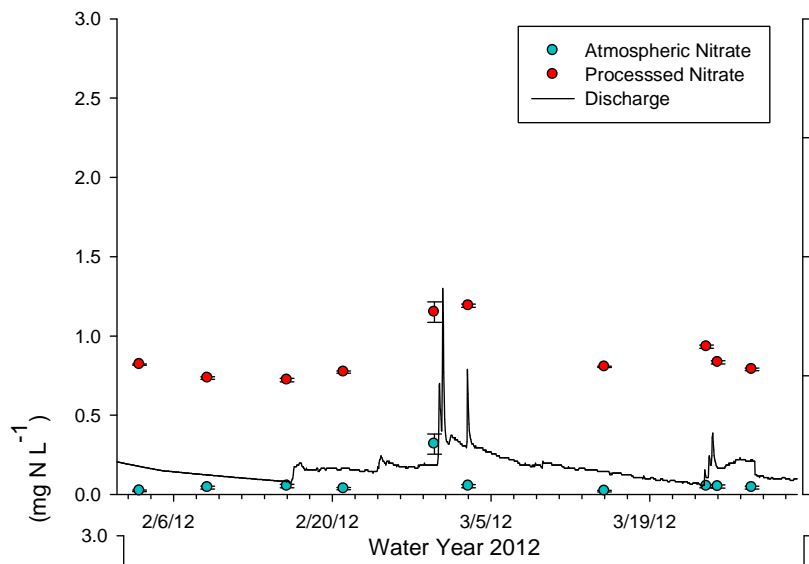


Figure A 1. Atmospheric  $\text{NO}_3\text{-N}$  concentrations (blue dots), and processed  $\text{NO}_3\text{-N}$  concentrations (red dots) at two month intervals. Error bars represent maximum and minimum range of atmospheric and processed concentrations. Instantaneous discharge values (15-minute data) are also shown (black lines). (pp. 66-68)





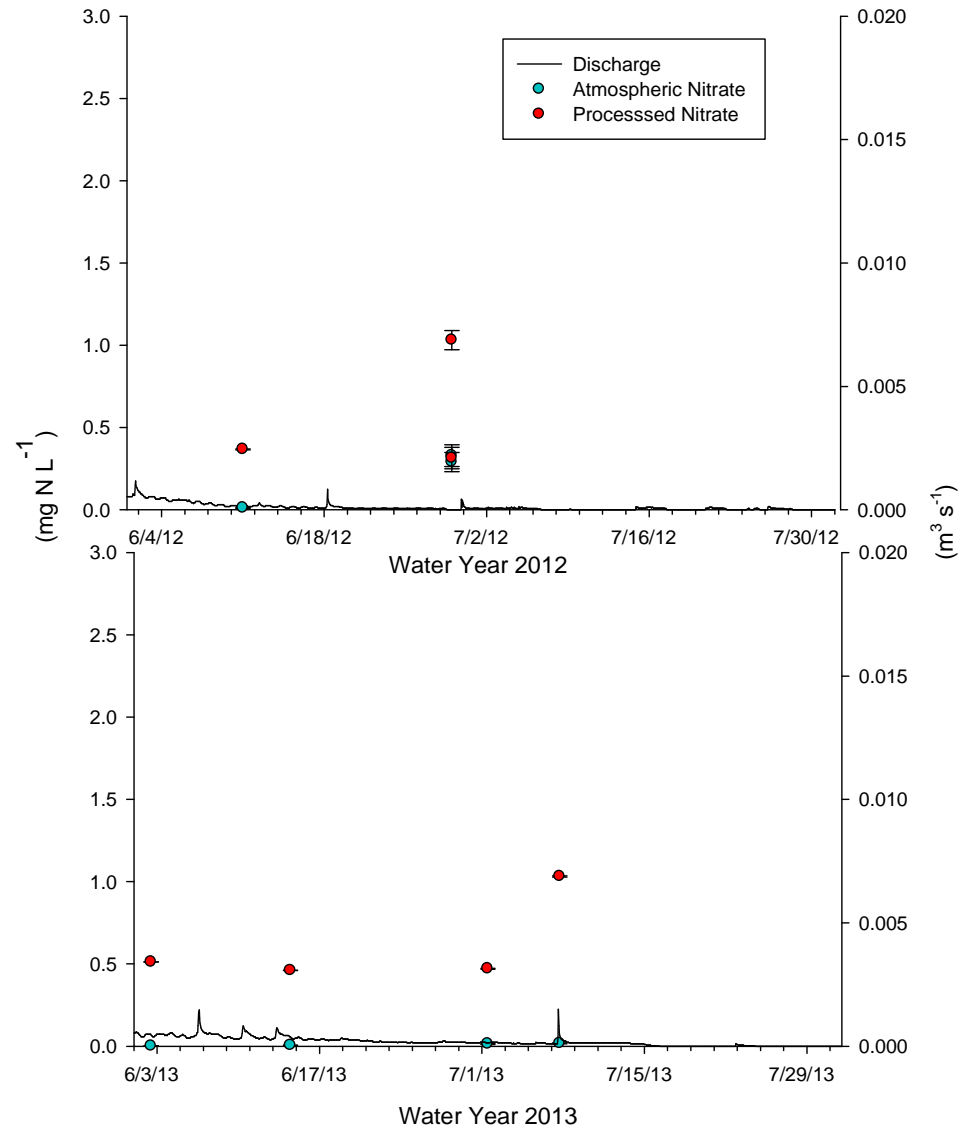


Table A 1. Displays monthly net mineralization and nitrification rates, nitrification to mineralization ratios, and annual rates within Oe/Oa and mineral horizons (MS) at TNEF for WY 2012.

Production of N (kg ha <sup>-1</sup> mo <sup>-1</sup> )	May	June	July	Aug.	Sept.	Oct.	ANOVA (p)
Net Ammonification Mineral Horizon	0.67	4.20	1.77	0.90	0.56	0.17	0.003
	0.42	1.98	1.08	0.45	0.43	0.49	
Net Nitrification Mineral Horizon	7.50	8.43	9.94	6.37	3.48	3.20	0.003
	2.01	1.79	1.92	0.88	0.78	0.98	
Net Mineralization Mineral Horizon	8.17	12.62	11.71	7.27	4.04	3.37	<.001
	2.24	2.31	2.68	1.07	0.70	0.89	
Net Ammonification Oe/Oa Horizon	2.12	3.07	3.97	4.86	2.23	0.97	0.140
	0.57	1.12	1.14	1.84	0.44	0.66	
Net Nitrification Oe/Oa Horizon	3.38	4.52	5.91	4.33	2.02	1.88	<.001
	0.52	0.55	1.12	0.62	0.35	0.31	
Net Mineralization Oe/Oa	5.50	7.59	9.88	9.19	4.26	2.85	<.001
	0.70	1.51	1.66	1.71	0.40	0.71	
Net Mineralization Oe/Oa+MS	13.67	20.21	21.59	16.46	8.29	6.22	<.001
	2.38	2.32	4.08	2.30	0.83	0.96	
Net Ammonification MS+Oe/Oa	2.79	7.26	5.74	5.75	2.79	1.14	0.014
	0.79	2.20	1.70	2.00	0.80	1.10	
Net Nitrification Oe/Oa + MS	10.89	12.95	15.85	10.70	5.50	5.08	<.001
	2.04	1.96	2.88	1.43	1.01	0.91	
Mineral Horizon RATIO	0.92	0.67	0.85	0.88	0.86	0.95	0.38
Oe/Oa RATIO	0.61	0.60	0.60	0.47	0.48	0.66	0.34
Combined Ratio	0.87	0.68	0.76	0.71	0.65	0.89	0.28
Net NH <sub>4</sub> -N /Net NO <sub>3</sub> -N	0.25	0.76	0.39	0.66	1.08	0.56	0.66
		Total NO <sub>3</sub> - N (kg ha <sup>-1</sup> )	60.9	Total NH <sub>4</sub> -N (kg ha <sup>-1</sup> )	25.47	Ratio (Nit/Min)	0.71
Net Mineralization (kg ha <sup>-1</sup> yr <sup>-1</sup> )	86.4						

Table A 2. Monthly standing pools of NH<sub>4</sub>-N, NO<sub>3</sub>-N, and IN within the Oe/Oa and mineral horizons at TNEF for WY 2012.

Standing Pool of N (kg ha <sup>-1</sup> )	May	June	July	August	September	October	ANOVA (p)		
NH <sub>4</sub> -N Mineral Horizon	1.84	1.53	1.58	1.24	1.95	1.73	0.25*		
	0.25	0.26	0.18	0.16	0.33	0.34			
NO <sub>3</sub> -N Mineral Horizon	0.52	0.33	0.70	0.90	1.14	1.83	0.018*		
	0.10	0.08	0.20	0.18	0.26	0.56			
IN Mineral Horizon	2.36	1.85	2.28	2.15	3.09	3.55	0.032*		
	0.31	0.25	0.26	0.29	0.49	0.70			
NH <sub>4</sub> -N Oe/Oa Horizon	1.19	0.84	1.13	2.20	1.38	1.49	0.65*		
	0.22	0.19	0.34	1.05	0.30	0.42			
NO <sub>3</sub> -N Oe/Oa Horizon	0.40	0.19	0.36	0.52	0.68	0.73	0.002*		
	0.08	0.06	0.10	0.08	0.14	0.12			
IN Oe/Oa Horizon	1.59	1.03	1.49	2.71	2.06	2.22	0.15*		
	0.24	0.16	0.32	1.08	0.28	0.41			
IN Oe/Oa+MS	3.95	2.88	3.76	4.86	5.15	5.77	0.042*		
	0.53	0.27	0.50	1.24	0.68	0.77			
NH <sub>4</sub> -N Oe/Oa+MS	3.03	2.36	2.71	3.44	3.34	3.22	0.90*		
	0.43	0.36	0.47	1.09	0.58	0.63			
NO <sub>3</sub> -N Oe/Oa+MS	0.92	0.52	1.05	1.42	1.81	2.55	0.002*		
	0.16	0.11	0.29	0.21	0.36	0.59			
				Net NH <sub>4</sub> -N	0.19	Net NO <sub>3</sub> -N	1.63	Net IN	1.82

Table A 3. Monthly fluxes of NH<sub>4</sub>-N, NO<sub>3</sub>-N, and IN within the top ten cm of mineral soil at TNEF for WY 2012.

Net Flux of N (kg ha <sup>-1</sup> mo <sup>-1</sup> )	NH <sub>4</sub> -N Top 10 cm	NO <sub>3</sub> -N top 10 cm	IN Top 10 cm
May	3.95	11.58	15.53
June	7.38	12.74	20.12
July	5.12	15.67	20.79
August	5.93	10.48	16.41
September	2.94	4.80	7.74
October*	1.34	2.54	3.88
Net NH <sub>4</sub> -N Flux	25.32	Net NO <sub>3</sub> -N Flux	55.26
Net IN Flux	80.58		

Table A 4. Seasonal loads ( $\text{kg ha}^{-1} \text{ yr}^{-1}$ ) and depth-weighted concentrations ( $\text{mg N L}^{-1}$ ) of  $\text{NH}_4\text{-N}$ ,  $\text{NO}_3\text{-N}$ , TN and IN from precipitation at TNEF for WY 2012-2013.

	TN Load	$\text{NH}_4\text{-N}$ Load	$\text{NO}_3\text{-N}$ Load	IN Load	Conc. $\text{NH}_4\text{-N}$	Conc. $\text{NO}_3\text{-N}$	Conc. IN	Conc. TN	Precip. (mm)
Fall-Winter WY 2012	4.72	1.39	1.15	2.55	0.27	0.23	0.50	0.92	511.
Spring-Summer WY 2012	2.94	0.95	0.89	1.85	0.19	0.17	0.36	0.57	512
Fall-Winter WY 2013	2.74	0.86	1.39	2.26	0.19	0.30	0.49	0.59	461
Spring-Summer WY 2013	2.17	0.68	0.56	1.25	0.12	0.10	0.23	0.40	543
WY 2012 Totals	7.66	2.34	2.04	4.40	0.23	0.20	0.43	0.75	1024
WY 2013 Totals	4.91	1.54	1.95	3.50	0.15	0.20	0.35	0.49	1004

Table A 5. Monthly runoff, yields and volume-weighted concentrations of NH<sub>4</sub>-N, NO<sub>3</sub>-N, and DON from the stream at TNEF for WY 2012-2013.

Year	m mo <sup>-1</sup> (runoff)	NO <sub>3</sub> -N Yield	NO <sub>3</sub> -N Conc.	NH <sub>4</sub> -N Yield	NH <sub>4</sub> -N Conc.	DON Yield	DON Conc.
Oct-11	0.02	0.14	0.60	0.00	0.00	0.01	0.06
Nov-11	0.06	0.47	0.82	0.00	0.00	0.03	0.05
Dec-11	0.06	0.59	1.02	0.00	0.00	0.05	0.09
Jan-12	0.07	0.77	1.15	0.00	0.00	0.05	0.07
Feb-12	0.05	0.50	0.95	0.00	0.00	0.04	0.08
Mar-12	0.05	0.50	1.04	0.00	0.00	0.04	0.07
Apr-12	0.03	0.24	0.72	0.00	0.00	0.02	0.06
May-12	0.02	0.13	0.65	0.00	0.00	0.01	0.05
Jun-12	0.00	0.01	0.48	0.00	0.00	0.00	0.04
Jul-12	0.00	0.00		0.00		0.00	
Aug-12	0.00	0.00		0.00		0.00	
Sep-12	0.00	0.00		0.00		0.00	
Oct-12	0.01	0.21	2.35	0.00	0.01	0.03	0.34
Nov-12	0.03	0.35	1.06	0.00	0.00	0.03	0.09
Dec-12	0.05	0.44	0.93	0.00	0.00	0.05	0.11
Jan-13	0.08	0.83	1.02	0.00	0.00	0.01	0.02
Feb-13	0.09	0.88	1.01	0.00	0.00	0.02	0.02
Mar-13	0.08	0.74	0.90	0.00	0.00	0.02	0.02
Apr-13	0.12	1.08	0.92	0.00	0.00	0.03	0.02
May-13	0.10	0.82	0.83	0.00	0.00	0.03	0.03
Jun-13	0.00	0.03	0.53	0.00	0.00	0.00	0.04
Jul-13	0.00	0.00	1.00	0.00	0.00	0.00	0.50
Aug-13	0.00	0.02	0.75	0.00	0.00	0.01	0.25
Sep-13	0.00	0.00	0.50	0.00	0.00	0.00	0.17
<hr/>							
2012							
Total	0.36	3.34	0.93	0.01	0.00	0.25	0.07
2013							
Total	0.57	5.41	0.95	0.02	0.00	0.24	0.04

Table A 6. Monthly runoff, yields and volume-weighted concentrations of atmospheric and processed NO<sub>3</sub>-N ( $\Delta O17=20$ ) from the stream at TNEF for WY 2012-2013.

Year	m mo <sup>-1</sup> (runoff)	Atm. Yield NO <sub>3</sub> -N	Atm. Conc. 20 NO <sub>3</sub> -N	Proc. Yield 20 NO <sub>3</sub> -N	Proc. Conc. 20 NO <sub>3</sub> -N
Oct-11	0.02	0.0070	0.0311	0.1290	0.5733
Nov-11	0.06	0.0420	0.0727	0.4580	0.7924
Dec-11	0.06	0.0110	0.0190	0.6140	1.0604
Jan-12	0.07	0.0390	0.0579	0.7310	1.0846
Feb-12	0.05	0.0610	0.1153	0.4390	0.8299
Mar-12	0.05	0.0330	0.0693	0.4670	0.9811
Apr-12	0.03	0.0080	0.0244	0.2270	0.6921
May-12	0.02	0.0200	0.1031	0.1060	0.5464
Jun-12	0.00	0.0030	0.1200	0.0100	0.4000
Jul-12	0.00	0.0000		0.0000	
Aug-12	0.00	0.0000		0.0000	
Sep-12	0.00	0.0000		0.0000	
Oct-12	0.01	0.0040	0.0440	0.0750	0.8242
Nov-12	0.03	0.0140	0.0428	0.3390	1.0367
Dec-12	0.05	0.0830	0.1758	0.3680	0.7797
Jan-13	0.08	0.1090	0.1334	0.7450	0.9119
Feb-13	0.09	0.1390	0.1583	0.6980	0.7950
Mar-13	0.08	0.2090	0.2539	0.4520	0.5492
Apr-13	0.12	0.0770	0.0653	0.9520	0.8068
May-13	0.10	0.0440	0.0443	0.7840	0.7895
Jun-13	0.00	0.0000	0.0000	0.0210	0.4286
Jul-13	0.00	0.0000	0.0000	0.0020	1.0000
Aug-13	0.00				
Sep-13	0.00				
2012	0.36	0.2240	0.0621	3.1810	0.8817
Total					
2013	0.57	0.6790	0.1206	4.4360	0.7876
Total					

Table A 7. Monthly runoff, yields and volume-weighted concentrations of atmospheric and processed NO<sub>3</sub>-N ( $\Delta O17=30$ ) from the stream at TNEF for WY 2012-2013.

Year	m mo <sup>-1</sup> (runoff)	Atm. Yield NO <sub>3</sub> -N	Atm. Conc. NO <sub>3</sub> -N	Proc. Yield NO <sub>3</sub> -N	Proc. Conc. NO <sub>3</sub> -N
Oct-11	0.02	0.0050	0.0222	0.1310	0.5822
Nov-11	0.06	0.0280	0.0484	0.4720	0.8166
Dec-11	0.06	0.0070	0.0121	0.6180	1.0674
Jan-12	0.07	0.0240	0.0356	0.7430	1.1024
Feb-12	0.05	0.0390	0.0737	0.4610	0.8715
Mar-12	0.05	0.0220	0.0462	0.4800	1.0084
Apr-12	0.03	0.0060	0.0183	0.2300	0.7012
May-12	0.02	0.0130	0.0670	0.1130	0.5825
Jun-12	0.00	0.0020	0.0800	0.0110	0.4400
Jul-12	0.00	0.0000		0.0000	
Aug-12	0.00	0.0000		0.0000	
Sep-12	0.00	0.0000		0.0000	
Oct-12	0.01	0.0030	0.0330	0.0760	0.8352
Nov-12	0.03	0.0090	0.0275	0.3430	1.0489
Dec-12	0.05	0.0560	0.1186	0.3950	0.8369
Jan-13	0.08	0.0730	0.0894	0.7800	0.9547
Feb-13	0.09	0.0930	0.1059	0.7450	0.8485
Mar-13	0.08	0.1410	0.1713	0.5190	0.6306
Apr-13	0.12	0.0510	0.0432	0.9780	0.8288
May-13	0.10	0.0300	0.0302	0.7980	0.8036
Jun-13	0.00	0.0000	0.0000	0.0210	0.4286
Jul-13	0.00	0.0000	0.0000	0.0020	1.0000
Aug-13	0.00				
Sep-13	0.00				
2012					
Total	0.36	0.1460	0.0405	3.2590	0.9033
2013					
Total	0.57	0.4560	0.0810	4.6570	0.8269



Table A 8. Grab sample concentration (mg N L<sup>-1</sup>) from the stream at TNEF for WY 2012-2013.

DATE	TDN	NH <sub>4</sub> -N	NO <sub>2</sub> -N	NO <sub>3</sub> -N	Atm. NO <sub>3</sub> -N 20	Proc. NO <sub>3</sub> -N 20	Atm. NO <sub>3</sub> -N 30	Proc. NO <sub>3</sub> -N 30
09/07/11	1.3288	0.0068	0.0000	1.0882				
10/01/11	0.9681	0.0467	0.0035	0.4967	0.0142	0.4860	0.0095	0.4907
10/02/11	0.7013	0.0016	0.0000	0.6147	0.0000	0.6148	0.0000	0.6148
10/07/11	0.5891	0.0040	0.0000	0.4935	0.0035	0.4900	0.0024	0.4911
10/13/11	0.8194	0.0030	0.0000	0.7462	0.0392	0.7070	0.0261	0.7201
10/20/11	0.6804	0.0035	0.0000	0.6223	0.0158	0.6065	0.0106	0.6117
10/28/11	0.5866	0.0027	0.0009	0.5349	0.0409	0.4949	0.0273	0.5085
11/10/11	0.6656	0.0034	0.0000	0.6290	0.1560	0.4730	0.1040	0.5250
11/20/11	0.7144	0.0026	0.0000	0.6677	0.0371	0.6306	0.0247	0.6430
11/23/11	1.2161	0.0040	0.0005	1.1608	0.0528	1.1085	0.0352	1.1261
12/05/11	0.8578	0.0032	0.0008	0.7221				
12/07/11	1.4050	0.0055	0.0008	1.1917	0.0000	1.1976	0.0000	1.1959
12/12/11	0.8974	0.0015	0.0003	0.8737	0.0244	0.8496	0.0162	0.8578
01/12/12	1.4825	0.0035	0.0006	1.3884	0.0493	1.3397	0.0329	1.3561
01/17/12	1.1735	0.0037	0.0011	1.0944	0.0640	1.0315	0.0427	1.0528
01/27/12	1.1193	0.0008	0.0009	1.0522	0.0711	0.9820	0.0474	1.0057
02/03/12	0.8997	0.0026	0.0012	0.8415	0.0273	0.8154	0.0182	0.8245
02/09/12	0.8344	0.0028	0.0011	0.7766	0.0521	0.7256	0.0348	0.7429
02/16/12	0.8950	0.0034	0.0000	0.7739	0.0636	0.7103	0.0424	0.7315
02/21/12	0.8521	0.0021	0.0000	0.8083	0.0439	0.7644	0.0292	0.7791
02/29/12	1.5739	0.0047	0.0011	1.4665	0.3808	1.0868	0.2539	1.2137
03/03/12	1.2658	0.0008	0.0011	1.2423	0.0630	1.1804	0.0420	1.2014
03/08/12	1.1524	0.0008	0.0000	0.9990				
03/15/12	0.9026	0.0007	0.0000	0.8260	0.0257	0.8003	0.0171	0.8089
03/24/12	1.0882	0.0046	0.0003	0.9835	0.0618	0.9220	0.0412	0.9426
03/25/12	0.9284	0.0039	0.0000	0.8831	0.0593	0.8238	0.0396	0.8435
03/28/12	0.8659	0.0040	0.0011	0.8319	0.0526	0.7804	0.0351	0.7979
04/05/12	0.8076	0.0030	0.0009	0.7505				
04/13/12	0.7279	0.0032	0.0012	0.6696	0.0086	0.6622	0.0057	0.6651
04/20/12	0.6817	0.0041	0.0013	0.6192	0.0049	0.6156	0.0033	0.6172
05/01/12	0.7377	0.0038	0.0007	0.6507	0.2746	0.3768	0.1831	0.4683
05/05/12	0.7031	0.0043	0.0010	0.5737	0.2252	0.3495	0.1502	0.4245
05/09/12	0.6038	0.0029	0.0025	0.5543	0.0160	0.5408	0.0107	0.5461
05/18/12	0.7170	0.0013	0.0006	0.6833	0.0253	0.6586	0.0169	0.6670
05/23/12	0.5940	0.0031	0.0000	0.5500	0.0103	0.5397	0.0069	0.5431
05/28/12	0.8950	0.0036	0.0009	0.8199	0.3394	0.4814	0.2263	0.5945
05/29/12	0.6047	0.0026	0.0002	0.5707	0.1610	0.4099	0.1073	0.4636
06/04/12	0.5076	0.0024	0.0014	0.4729				
06/11/12	0.4547	0.0047	0.0024	0.3758	0.0135	0.3647	0.0090	0.3692
06/19/12	0.4363	0.0054	0.0007	0.3822				
06/29/12	1.7408	0.0198	0.0017	1.3189	0.3478	0.9728	0.2319	1.0887
10/29/12	0.9482	0.0107	0.0015	0.4482	0.0397	0.4100	0.0265	0.4232
10/30/2012	1.5450	0.0059	0.0002	1.3442	0.0486	1.2958	0.0324	1.3120
10/31/12	1.3728	0.0050	0.0000	1.2273	0.0435	1.2401	0.0267	1.2006
11/01/12	1.1929	0.0037	0.0000	1.0615				
11/02/12	1.2555	0.0039	0.0000	1.1326	0.0607	1.0719	0.0405	1.0921
11/03/12	1.2603	0.0042	0.0000	1.1413				
11/04/12	1.2401	0.0028	0.0000	1.1360				
11/06/12	1.2278	0.0029	0.0000	1.1172	0.0373	1.0799	0.0249	1.0923
11/12/12	1.3019	0.0016	0.0000	1.1532	0.0623	1.0909	0.0415	1.1117
11/19/12	1.0182	0.0012	0.0000	0.9878	0.0392	0.9486	0.0261	0.9617
11/26/12	0.8713	0.0024	0.0000	0.8277				
12/04/12	0.8270	0.0020	0.0000	0.7656				
12/12/12	1.1064	0.0024	0.0007	1.0327	0.0225	1.0109	0.0150	1.0184
12/20/12	1.1724	0.0018	0.0000	0.8749	0.2984	0.5765	0.1990	0.6759
12/24/12	0.9995	0.0018	0.0000	0.9635	0.3407	0.6228	0.2271	0.7364
01/03/13	0.8659	0.0014	0.0034	0.8249	0.0332	0.7951	0.0222	0.8061
01/10/13	0.8250	0.0014	0.0000	0.8146	0.3586	0.4560	0.2391	0.5755
01/14/13	1.2301	0.0023	0.0022	1.2066	0.1138	1.0950	0.0759	1.1329
01/24/13	0.9324	0.0019	0.0014	0.9131				
01/28/13	0.8711	0.0027	0.0000	0.8600	0.0952	0.7648	0.0635	0.7965
01/30/13	0.9779	0.0064	0.0001	0.9306				
01/31/13	1.3677	0.0037	0.0015	1.3470	0.0845	1.2640	0.0564	1.2921

02/08/13	0.9656	0.0030	0.0000	0.9309	0.2571	0.6738	0.1714	0.7595
02/14/13	0.9225	0.0003	0.0032	0.8935	0.0689	0.8278	0.0459	0.8508
02/27/13	1.0412	0.0032	0.0014	1.0257				
03/05/13	0.8526	0.0017	0.0002	0.8059				
03/10/13	0.8171	0.0027	0.0043	0.7544	0.3409	0.4178	0.2273	0.5314
03/22/13	0.9612	0.0015	0.0019	0.9654				
04/04/13	1.0723	0.0019	0.0001	1.0499				
04/11/13	0.9196	0.0028	0.0006	0.9112	0.0416	0.8702	0.0277	0.8841
04/15/13	1.0247	0.0020	0.0000	1.0002	0.0459	0.9543	0.0306	0.9696
04/22/13	0.8080	0.0008	0.0000	0.8087				
04/24/13	0.8155	0.0030	0.0000	0.7616	0.0550	0.7066	0.0367	0.7249
05/05/13	0.6361	0.0038	0.0036	0.6094	0.0171	0.5959	0.0114	0.6016
05/08/13	1.1568	0.0051	0.0037	1.1075	0.0732	1.0380	0.0488	1.0624
05/15/13	0.7863	0.0029	0.0007	0.7374	0.0388	0.6993	0.0259	0.7122
05/24/13	0.5946	0.0046	0.0028	0.5830				
06/02/13	0.5510	0.0048	0.0014	0.5125	0.0019	0.5120	0.0013	0.5126
06/07/13	0.6518	0.0077	0.0017	0.5645				
06/14/13	0.4925	0.0057	0.0002	0.4658	0.0067	0.4593	0.0045	0.4615
06/25/13	0.4187	0.0073	0.0000	0.2976				
07/01/13	0.6272	0.0048	0.0000	0.4858	0.0173	0.4685	0.0115	0.4743
07/07/13	1.4272	0.0111	0.0009	1.0480	0.0209	1.0280	0.0140	1.0349
08/23/13	1.0111	0.0059	0.0010	0.781				
09/10/13	0.5171	0.0065	0.0006	0.4074				

Table A 9. Isotopic signatures for NO<sub>3</sub>-N from the stream at TNEF for WY 2012-2013, along with calculated atmospheric and processes proportions present in the total NO<sub>3</sub>-N concentration.

Date	Time	NO <sub>3</sub> -N Conc. (mg N L <sup>-1</sup> )	δ <sup>17</sup> O	δ <sup>18</sup> O	δ <sup>15</sup> N	Δ <sup>17</sup> O	% Atm.
09/07/11	12:00	1.09					
10/01/11	11:00	0.50	-2.65	-6.19	4.15	0.57	2.85
10/02/11	13:15	0.61	-0.92	-1.76	0.93	0.00	-0.02
10/07/11	15:00	0.49	-2.17	-4.45	1.50	0.14	0.71
10/13/11	12:00	0.75	1.02	-0.06	3.95	1.05	5.25
10/20/11	12:00	0.62	-0.21	-1.38	0.97	0.51	2.55
10/28/11	13:45	0.54	1.98	0.88	4.88	1.53	7.64
11/10/11	12:00	0.63	8.74	7.26	5.28	4.96	24.80
11/20/11	12:00	0.67	1.95	1.60	1.58	1.11	5.55
11/23/11	12:00	1.16	1.05	0.28	0.39	0.91	4.55
12/07/11	12:00	1.19	0.59	1.30	-0.23	-0.09	-0.43
12/12/11	12:00	0.87	0.91	0.68	0.50	0.56	2.79
01/12/12	12:00	1.39	2.33	3.11	-0.16	0.71	3.55
01/17/12	12:00	1.10	2.95	3.42	0.63	1.17	5.84
01/27/12	12:00	1.05	2.18	1.59	0.05	1.35	6.75
02/03/12	12:00	0.84	2.18	2.94	1.00	0.65	3.24
02/09/12	12:00	0.78	2.18	1.61	0.87	1.34	6.70
02/16/12	12:00	0.77	5.80	7.99	1.42	1.64	8.21
02/21/12	12:00	0.81	2.86	3.41	1.36	1.09	5.43
02/29/12	12:00	1.47	2.88	-4.43	4.45	5.19	25.95
03/03/12	12:00	1.24	3.51	4.81	0.51	1.01	5.07
03/15/12	12:00	0.83	2.79	4.17	1.17	0.62	3.11
03/24/12	12:00	0.98	3.43	4.17	1.10	1.26	6.29
03/25/12	12:00	0.88	3.62	4.37	1.53	1.34	6.72
03/28/12	12:00	0.83	2.86	3.07	1.23	1.26	6.31
04/05/12	12:00	0.75					
04/13/12	12:00	0.67	2.40	4.13	2.13	0.25	1.27
04/20/12	12:00	0.62	1.56	2.69	2.10	0.16	0.80
05/01/12	12:00	0.65	7.57	-1.65	4.18	8.43	42.15
05/05/12	12:00	0.57	10.09	4.34	4.93	7.84	39.19
05/09/12	12:00	0.56	1.22	1.25	2.65	0.57	2.87
05/18/12	12:00	0.68	2.45	3.29	2.47	0.74	3.70
05/23/12	12:00	0.55	0.30	-0.14	1.59	0.37	1.87
05/28/12	12:00	0.82	9.52	2.40	5.92	8.27	41.35
05/29/12	12:00	0.57	6.11	0.91	4.38	5.64	28.20
06/04/12	12:00	0.47					
06/11/12	12:00	0.38	-1.86	-4.96	3.14	0.72	3.58
06/19/12	12:00	0.38					
06/29/12	22:00	0.64	13.34	2.05	8.83	12.28	61.39
06/29/12	22:30	1.32	11.68	12.34	-1.32	5.27	26.34
10/29/12	15:10	0.45	6.99	10.04	0.94	1.77	8.84
10/29/12	17:10	2.84	2.91	4.03	-0.72	0.81	4.07
10/29/12	19:10	1.95	2.03	2.96	-1.31	0.49	2.46
10/29/12	21:10	1.57	2.51	3.55	-0.23	0.66	3.31

10/29/12	23:10	1.33	2.81	4.04	-0.30	0.71	3.56
10/30/12	1:10	1.39	0.24	-1.28	-1.35	0.91	4.55
10/30/12	3:10	1.38					
10/30/12	5:10	1.36					
10/30/12	7:10	1.36	0.18	-0.60	-1.10	0.50	2.48
10/30/12	9:10	1.37					
10/30/12	11:10	1.38	-0.50	-1.00	-1.17	0.02	0.08
10/30/12	15:10	1.38					
10/30/12	19:10	1.34	-0.27	-1.91	-0.76	0.72	3.62
10/30/12	23:10	1.32					
10/31/12	3:10	1.28	0.58	-0.19	-0.32	0.68	3.39
10/31/12	7:10	1.26					
10/31/12	11:10	1.23	1.02	0.71	0.11	0.65	3.26
10/31/12	13:10	1.18					
10/31/12	16:00	1.16					
11/01/12	15:45	1.06					
11/02/12	13:30	1.13	1.77	1.33	0.64	1.07	5.36
11/03/12	19:00	1.14					
11/04/12	15:45	1.14					
11/06/12	18:30	1.12	0.18	-0.93	0.40	0.67	3.34
11/12/12	12:00	1.15	2.80	3.31	4.37	1.08	5.40
11/19/2012	12:00	0.99	3.99	6.15	0.15	0.79	3.97
12/4/2012	12:00	0.77					
12/12/2012	15:50	1.03	0.03	-0.77	1.40	0.44	2.18
12/20/2012	11:40	0.87	2.79	-7.75	4.21	6.82	34.11
12/24/2012	12:00	0.96	5.26	-3.48	6.78	7.07	35.36
1/3/2013	16:45	0.83	1.85	2.02	1.55	0.80	4.01
1/10/2013	12:00	0.81	9.04	0.45	5.06	8.81	44.03
1/14/2013	17:10	1.21	3.90	3.87	0.59	1.88	9.41
1/24/2013	12:00	0.91					
1/28/2013	12:00	0.86	5.16	5.67	1.61	2.21	11.07
1/30/2013	14:00	0.93					
1/31/2013	14:45	1.35	2.84	3.05	0.24	1.25	6.27
2/8/2013	12:00	0.93	6.15	1.21	4.90	5.52	27.62
2/14/2013	12:00	0.90	3.91	4.56	1.26	1.54	7.68
2/27/2013	17:00	1.03	4.71	4.34	0.63	2.46	12.29
3/5/2013	12:00	0.81					
3/10/2013	18:00	0.76	8.74	-0.48	4.94	8.99	44.93
3/22/2013	15:30	0.97	2.93	3.49	1.06	1.12	5.58
4/4/2013	12:00	1.05					
4/11/2013	12:00	0.91	3.27	4.54	1.18	0.91	4.56
4/15/2013	17:30	1.00	3.42	4.81	1.31	0.92	4.59
4/22/2013	12:00	0.81					
4/24/2013	12:00	0.76	4.47	5.81	1.39	1.45	7.23
5/5/2013	12:00	0.61	2.68	4.08	1.90	0.56	2.78
5/8/2013	12:00	1.11	3.47	4.13	0.71	1.32	6.59
5/15/2013	17:30	0.74	1.49	0.85	0.92	1.05	5.26
5/24/2013	12:00	0.59					
6/2/2013	12:00	0.51	-2.18	-4.34	3.07	0.07	0.37
6/7/2013	12:00	0.57					

6/14/2013	12:00	0.47	-0.77	-2.03	2.56	0.29	1.44
6/25/2013	12:00	0.30					
7/1/2013	12:00	0.49	-0.36	-2.05	3.55	0.71	3.56
7/7/2013	17:00	1.05	-0.78	-2.27	0.43	0.40	2.00

---

Table A 10. Monthly net nitrification and mineralization rates ( $\text{g m}^{-2} \text{mo}^{-2}$ ) within the the top 10 cm of mineral soil at TNEF. Sections are split up by months and have subsection that display within and inter-plot variability. FF stands for Oe/Oa horizon.

May	<i>Plot Variability</i>				June	<i>Plot Variability</i>			
	Min.	S.E.	Nit.	S.E.		Min	S.E.	Nit.	S.E.
1ff	0.69	0.10	0.48	0.03	1ff	1.03	0.38	0.52	0.13
2ff	0.45	0.12	0.17	0.06	2ff	0.72	0.24	0.43	0.12
3ff	0.51	0.14	0.36	0.07	3ff	0.52	0.08	0.40	0.04
1ms	0.44	0.06	0.37	0.07	1ms	0.50	0.16	0.45	0.12
2ms	1.16	0.19	1.01	0.16	2ms	1.85	0.21	0.76	0.26
3ms	0.85	0.66	0.87	0.58	3ms	1.44	0.31	1.32	0.33
FF	0.55	0.07	0.34	0.09	FF	0.76	0.15	0.45	0.04
MS	0.82	0.21	0.75	0.19	MS	1.27	0.40	0.85	0.26
<i>Interplot Variability</i>					<i>Interplot Variability</i>				
	Min.	S.E.	Nit.	S.E.		Min.	S.E.	Nit.	S.E.
FF	0.55	0.07	0.34	0.09	FF	0.76	0.15	0.45	0.04
MS	0.82	0.21	0.75	0.19	MS	1.26	0.40	0.84	0.26
July	<i>Plot Variability</i>				August	<i>Plot Variability</i>			

	Min.	S.E.	Nit.	S.E.		Min.	S.E.	Nit.	S.E.
1ff	0.71	0.13	0.44	0.14	1ff	0.84	0.25	0.42	0.07
2ff	1.35	0.23	0.77	0.27	2ff	1.29	0.34	0.40	0.15
3ff	0.90	0.39	0.56	0.17	3ff	0.63	0.24	0.48	0.14
1ms	0.43	0.10	0.42	0.10	1ms	0.68	0.10	0.54	0.05
2ms	1.71	0.55	1.21	0.31	2ms	0.78	0.25	0.64	0.14
3ms	1.38	0.33	1.35	0.29	3ms	0.72	0.25	0.73	0.25
FF	0.99	0.19	0.59	0.10	FF	0.92	0.19	0.43	0.02
MS	1.17	0.38	0.99	0.29	MS	0.73	0.03	0.64	0.05
<i>Interplot Variability</i>					<i>Interplot Variability</i>				
	Min.	S.E.	Nit.	S.E.		Min.	S.E.	Nit.	S.E.
FF	0.99	0.19	0.59	0.10	FF	0.92	0.19	0.43	0.02
MS	1.17	0.38	0.99	0.29	MS	0.73	0.03	0.64	0.05
<i>Sept. Plot Variability</i>					<i>Oct. Plot Variability</i>				
	Min.	S.E.	Nit.	S.E.		Min.	S.E.	Nit.	S.E.
1ff	0.43	0.11	0.20	0.05	1ff	0.21	0.09	0.15	0.02

2ff	0.39	0.06	0.15	0.07	2ff	0.44	0.17	0.21	0.05
3ff	0.45	0.05	0.26	0.06	3ff	0.20	0.06	0.20	0.09
1ms	0.16	0.02	0.14	0.02	1ms	0.18	0.08	0.16	0.07
2ms	0.47	0.09	0.32	0.15	2ms	0.27	0.10	0.16	0.12
3ms	0.58	0.06	0.58	0.04	3ms	0.56	0.20	0.63	0.15
FF	0.43	0.02	0.20	0.03	FF	0.28	0.08	0.19	0.02
MS	0.40	0.12	0.35	0.13	MS	0.34	0.12	0.32	0.16
<i>Interplot Variability</i>					<i>Interplot Variability</i>				
	Min.	S.E.	Nit.	S.E.		Min.	S.E.	Nit.	S.E.
FF	0.43	0.02	0.20	0.03	FF	0.28	0.08	0.19	0.02
MS	0.40	0.13	0.35	0.13	MS	0.34	0.12	0.32	0.16



Table A 11. Results generated from the spring sampling isotopic approach (eq. 22) relying on the March 22, 2013 spring stream sample and annual IN concentration/deposition data from water year 2012.

<i>d</i> (%)	Measured Deposition (kg ha <sup>-1</sup> yr <sup>-1</sup> )	Measured 2012 Depth- weighted IN Conc.	Measured Spring 2013 Stream NO <sub>3</sub> -N atm Conc.	Estimated Absolute Difference	<i>a</i>
0%	5.6	0.45	0.054	0.396	0.88
60%	5.6	0.18	0.054	0.126	0.70
80%	5.6	0.09	0.054	0.036	0.40
83%	5.6	0.076	0.054	0.023	0.29
87%	5.6	0.059	0.054	0.005	0.08
	Estimated Mineralization (kg ha <sup>-1</sup> yr <sup>-1</sup> )	Measured Spring 2013 Stream NO <sub>3</sub> -N proc Conc.	<i>Pa</i>	<i>Pp</i>	
	94.71	0.913	0.06	0.94	

## Literature Cited

- Aber, John D., Christine L. Goodale, Scott V. Ollinger, Jennifer E Smith, Alison H. Magill, Mary E. Martin, Richard A. Hallet, and John L. Stoddard. 2003. "Is Nitrogen Deposition Altering the Nitrogen Status of Northeastern Forests?" *BioScience* 53 (4): 375–89.
- Aber, John D., William McDowell, Knute Nadelhoffer, Alison Magill, Glenn Berntson, Mark Kamakea, Steven McNulty, William Currie, Lindsey Rustad, and Ivan Fernandez. 1998. "Nitrogen Saturation in Temperate Forest Ecosystems." *BioScience* 48 (11): 921–34. doi:10.2307/1313296.
- Aber, John D., Knute J. Nadelhoffer, Paul Steudler, and Jerry M. Melillo. 1989. "Nitrogen Saturation in Northern Forest Ecosystems." *BioScience* 39 (6): 378–86. doi:10.2307/1311067.
- Ågren, Göran I., and Ernesto Bosatta. 1988. "Nitrogen Saturation of Terrestrial Ecosystems." *Environmental Pollution* 54 (3–4): 185–97. doi:10.1016/0269-7491(88)90111-X.
- Band, L. E., C. L. Tague, P. Groffman, and K. Belt. 2001. "Forest Ecosystem Processes at the Watershed Scale: Hydrological and Ecological Controls of Nitrogen Export." *Hydrological Processes* 15 (10): 2013–28. doi:10.1002/hyp.253.
- Bechtold, J. Scott, Rick T. Edwards, and Robert J. Naiman. 2003. "Biotic versus Hydrologic Control over Seasonal Nitrate Leaching in a Floodplain Forest." *Biogeochemistry* 63 (1): 53–72. doi:10.1023/A:1023350127042.
- Bernal, Susana, Lars O. Hedin, Gene E. Likens, Stefan Gerber, and Don C. Buso. 2012. "Complex Response of the Forest Nitrogen Cycle to Climate Change."

*Proceedings of the National Academy of Sciences* 109 (9): 3406–11.

doi:10.1073/pnas.1121448109.

- Boesch, DF, Brinsfield, RB, and Magnien, RE. 2001. “Chesapeake Bay Eutrophication: Scientific Understanding, Ecosystem Restoration, and Challenges for Agriculture.” *Journal of Environmental Quality* 30 (2).
- Boyer, Elizabeth W., George M. Hornberger, Kenneth E. Bencala, and Diane M. McKnight. 1997. “Response Characteristics of DOC Flushing in an Alpine Catchment.” *Hydrological Processes* 11 (12): 1635–47. doi:10.1002/(SICI)1099-1085(19971015)11:12<1635::AID-HYP494>3.0.CO;2-H.
- Bredemeier, M., A. Dohrenbusch, and D. Murach. 1995. “Response of Soil Water Chemistry and Fine-Roots to Clean Rain in a Spruce Forest Ecosystem at Solling, FRG.” *Water, Air, and Soil Pollution* 85 (3): 1605–11. doi:10.1007/BF00477210.
- Brookshire, E. N, Stefan Gerber, Jackson R Webster, James M Vose, and Wayne T Swank. 2011. “Direct Effects of Temperature on Forest Nitrogen Cycling Revealed through Analysis of Long-term Watershed Records.” *Global Change Biology* 17 (1): 297–308. doi:10.1111/j.1365-2486.2010.02245.x.
- Buda, Anthony R., and David R. DeWalle. 2009. “Dynamics of Stream Nitrate Sources and Flow Pathways during Stormflows on Urban, Forest and Agricultural Watersheds in Central Pennsylvania, USA.” *Hydrological Processes* 23 (23): 3292–3305. doi:10.1002/hyp.7423.
- Campbell, John L., James W. Hornbeck, Myron J. Mitchell, Mary Beth Adams, Mark S. Castro, Charles T. Driscoll, Jeffrey S. Kahl, et al. 2004. “Input-Output Budgets of Inorganic Nitrogen for 24 Forest Watersheds in the Northeastern United States: A

Review.” *Water, Air, & Soil Pollution* 151 (1-4): 373–96.

doi:10.1023/B:WATE.0000009908.94219.04.

Campbell, John L., Myron J. Mitchell, and Bernhard Mayer. 2006. “Isotopic Assessment of NO<sub>3</sub><sup>-</sup> and SO<sub>4</sub><sup>2-</sup> Mobility during Winter in Two Adjacent Watersheds in the Adirondack Mountains, New York.” *Journal of Geophysical Research* 111 (November): 15 PP. doi:200610.1029/2006JG000208.

Carter, M. R., and E. G. Gregorich. 2007. *Soil Sampling and Methods of Analysis, Second Edition*. CRC Press.

Castellano, Michael J., David Bruce Lewis, and Jason P. Kaye. 2013. “Response of Soil Nitrogen Retention to the Interactive Effects of Soil Texture, Hydrology, and Organic Matter.” *Journal of Geophysical Research: Biogeosciences* 118 (1): 280–90. doi:10.1002/jgrg.20015.

Castro, Mark S., and Charles T. Driscoll. 2002. “Atmospheric Nitrogen Deposition to Estuaries in the Mid-Atlantic and Northeastern United States.” *Environmental Science & Technology* 36 (15): 3242–49. doi:10.1021/es010664o.

Castro, Mark S., Keith N. Eshleman, Louis F. Pitelka, Geoff Frech, Molly Ramsey, William S. Currie, Karen Kuers, et al. 2007. “Symptoms of Nitrogen Saturation in an Aggrading Forested Watershed in Western Maryland.” *Biogeochemistry* 84 (3): 333–48. doi:10.1007/s10533-007-9125-z.

Cleveland, Cory C., and Daniel Liptzin. 2007. “C:N:P Stoichiometry in Soil: Is There a ‘Redfield Ratio’ for the Microbial Biomass?” *Biogeochemistry* 85 (3): 235–52. doi:10.1007/s10533-007-9132-0.

- Corre, Marife D., and Norbert P. Lamersdorf. 2004. "Reversal of Nitrogen Saturation after Long-Term Deposition Reduction: Impact on Soil Nitrogen Cycling." *Ecology* 85 (11): 3090–3104. doi:10.1890/03-0423.
- Costa, A. W., G. Michalski, A. J. Schauer, B. Alexander, E. J. Steig, and P. B. Shepson. 2011. "Analysis of Atmospheric Inputs of Nitrate to a Temperate Forest Ecosystem from  $\Delta^{17}\text{O}$  Isotope Ratio Measurements." *Geophysical Research Letters* 38 (15): n/a–n/a. doi:10.1029/2011GL047539.
- Elliott, Katherine J., Lindsay R. Boring, Wayne T. Swank, and Bruce R. Haines. 1997. "Successional Changes in Plant Species Diversity and Composition after Clearcutting a Southern Appalachian Watershed." *Forest Ecology and Management* 92 (1–3): 67–85. doi:10.1016/S0378-1127(96)03947-3.
- EPA, US. 2010. "Chesapeake Bay Phase 5.3 Community Watershed Model." *EPA 903S10002 - CBP/TRS-303-10. U.S. Environmental Protection Agency, Chesapeake Bay Program Office, Annapolis MD. December 2010*, no. 2010.
- Eshleman, Keith N., Kathleen M. Kline, Raymond P. Morgan II, Nancy M. Castro, and Timothy L. Negley. 2008. "Contemporary Trends in the Acid–Base Status of Two Acid-Sensitive Streams in Western Maryland." *Environmental Science & Technology* 42 (1): 56–61. doi:10.1021/es071195e.
- Eshleman, Keith N., Robert D. Sabo, and Kathleen M. Kline. 2013. "Surface Water Quality Is Improving due to Declining Atmospheric N Deposition." *Environmental Science & Technology*, October. doi:10.1021/es4028748. <http://dx.doi.org/10.1021/es4028748>.

- Fang, Yunting, Keisuke Koba, Akiko Makabe, Feifei Zhu, Shaoyan Fan, Xueyan Liu, and Muneoki Yoh. 2012. "Low  $\delta^{18}\text{O}$  Values of Nitrate Produced from Nitrification in Temperate Forest Soils." *Environmental Science & Technology* 46 (16): 8723–30. doi:10.1021/es300510r.
- Galloway, J., J. D. Aber, Jan Willem Erisman, Sybil P. Seitzinger, Robert W. Howarth, Ellis B. Cowling, and B. Jack Cosby. 2003. "The Nitrogen Cascade." *BioScience* 53 (4): 341–56. doi:10.1641/0006-3568(2003)053[0341:TNC]2.0.CO;2.
- Goodale, Christine L., John D. Aber, and Peter M. Vitousek. 2003. "An Unexpected Nitrate Decline in New Hampshire Streams." *Ecosystems* 6 (1): 75–86. doi:10.1007/s10021-002-0219-0.
- Goodale, Christine L., Steven A. Thomas, Guinevere Fredriksen, Emily M. Elliott, Kathryn M. Flinn, Thomas J. Butler, and M. Todd Walter. 2009. "Unusual Seasonal Patterns and Inferred Processes of Nitrogen Retention in Forested Headwaters of the Upper Susquehanna River." *Biogeochemistry* 93 (3): 197–218. doi:10.1007/s10533-009-9298-8.
- Hedin, Lars O., Juan J. Armesto, and Arthur H. Johnson. 1995. "Patterns of Nutrient Loss from Unpolluted, Old-Growth Temperate Forests: Evaluation of Biogeochemical Theory." *Ecology* 76 (2): 493–509. doi:10.2307/1941208.
- Hirsch, Robert M, Douglas L Moyer, and Stacey A Archfield. 2010. "Weighted Regressions on Time, Discharge, and Season (WRTDS), with an Application to Chesapeake Bay River Inputs." *Journal of the American Water Resources Association* 46 (5): 857–80. doi:10.1111/j.1752-1688.2010.00482.x.

- Hutchinson, G. Evelyn. 1948. "Circular Causal Systems in Ecology." *Annals of the New York Academy of Sciences* 50 (4): 221–46. doi:10.1111/j.1749-6632.1948.tb39854.x.
- Imсанде, J., and B. Touraine. 1994. "N Demand and the Regulation of Nitrate Uptake." *Plant Physiology* 105 (1): 3–7.
- Inamdar, Shreeram P., Sheila F. Christopher, and Myron J. Mitchell. 2004. "Export Mechanisms for Dissolved Organic Carbon and Nitrate during Summer Storm Events in a Glaciated Forested Catchment in New York, USA." *Hydrological Processes* 18 (14): 2651–61. doi:10.1002/hyp.5572.
- Judd, Kristin E., Gene E. Likens, and Peter M. Groffman. 2007. "High Nitrate Retention during Winter in Soils of the Hubbard Brook Experimental Forest." *Ecosystems* 10 (2): 217–25. doi:10.1007/s10021-007-9027-x.
- Kaushal, Sujay S., Peter M. Groffman, Lawrence E. Band, Catherine A. Shields, Raymond P. Morgan, Margaret A. Palmer, Kenneth T. Belt, Christopher M. Swan, Stuart E. G. Findlay, and Gary T. Fisher. 2008. "Interaction between Urbanization and Climate Variability Amplifies Watershed Nitrate Export in Maryland." *Environmental Science & Technology* 42 (16): 5872–78. doi:10.1021/es800264f.
- Knoepp, Jennifer D., and Wayne T. Swank. 1998. "Rates of Nitrogen Mineralization across an Elevation and Vegetation Gradient in the Southern Appalachians." *Plant and Soil* 204 (2): 235–41. doi:10.1023/A:1004375412512.

- Kothawala, Dolly N., Shaun A. Watmough, Martyn N. Futter, Leiming Zhang, and Peter J. Dillon. 2011. "Stream Nitrate Responds Rapidly to Decreasing Nitrate Deposition." *Ecosystems* 14 (2): 274–86. doi:10.1007/s10021-011-9422-1.
- McGroddy, Megan E., Tanguy Daufresne, and Lars O. Hedin. 2004. "Scaling of C:N:P Stoichiometry in Forests Worldwide: Implications of Terrestrial Redfield-Type Ratios." *Ecology* 85 (9): 2390–2401. doi:10.1890/03-0351.
- McLauchlan, Kendra K., Carolyn J Ferguson, Iris E Wilson, Troy W Ocheltree, and Joseph M Craine. 2010. "Thirteen Decades of Foliar Isotopes Indicate Declining Nitrogen Availability in Central North American Grasslands." *New Phytologist* 187 (4): 1135–45. doi:10.1111/j.1469-8137.2010.03322.x.
- McLauchlan, Kendra K., Joseph M. Craine, W. Wyatt Oswald, Peter R. Leavitt, and Gene E. Likens. 2007. "Changes in Nitrogen Cycling during the Past Century in a Northern Hardwood Forest." *Proceedings of the National Academy of Sciences* 104 (18): 7466–7470. doi:10.1073/pnas.0701779104.
- Meier, Albert J., Susan Power Bratton, and David Cameron Duffy. 1995. "Possible Ecological Mechanisms for Loss of Vernal-Herb Diversity in Logged Eastern Deciduous Forests." *Ecological Applications* 5 (4): 935–46. doi:10.2307/2269344.
- Michalski, Greg, Thomas Meixner, Mark Fenn, Larry Hernandez, Abby Sirulnik, Edith Allen, and Mark Thiemens. 2004. "Tracing Atmospheric Nitrate Deposition in a Complex Semiarid Ecosystem Using  $\Delta^{17}\text{O}$ ." *Environmental Science & Technology* 38 (7): 2175–81. doi:10.1021/es034980+.



- Morgan, Raymond P., and Kathleen M. Kline. 2011. "Nutrient Concentrations in Maryland Non-Tidal Streams." *Environmental Monitoring and Assessment* 178 (1-4): 221–35. doi:10.1007/s10661-010-1684-0.
- Nadelhoffer, Knute J., John D. Aber, and Jerry M. Melillo. 1984. "Seasonal Patterns of Ammonium and Nitrate Uptake in Nine Temperate Forest Ecosystems." *Plant and Soil* 80 (3): 321–35. doi:10.1007/BF02140039.
- Nadelhoffer, Knute J., and James W. Raich. 1992. "Fine Root Production Estimates and Belowground Carbon Allocation in Forest Ecosystems." *Ecology* 73 (4): 1139. doi:10.2307/1940664.
- Negley, Timothy L, and Keith N Eshleman. 2006. "Comparison of Stormflow Responses of Surface-mined and Forested Watersheds in the Appalachian Mountains, USA." *Hydrological Processes* 20 (16): 3467–83. doi:10.1002/hyp.6148.
- Ohte, N., S. D. Sebestyen, J. B. Shanley, D. H. Doctor, C. Kendall, S. D. Wankel, and E. W. Boyer. 2004. "Tracing Sources of Nitrate in Snowmelt Runoff Using a High-Resolution Isotopic Technique." *Geophysical Research Letters* 31 (21): L21506. doi:10.1029/2004GL020908.
- Pan, Yude, John Hom, Richard Birdsey, and Kevin McCullough. 2004. "Impacts of Rising Nitrogen Deposition on N Exports from Forests to Surface Waters in the Chesapeake Bay Watershed." *Environmental Management* 33 (1): S120–S131. doi:10.1007/s00267-003-9122-5.
- Pastor, John, John D. Aber, Charles A. McClaugherty, and Jerry M. Melillo. 1984. "Aboveground Production and N and P Cycling Along a Nitrogen Mineralization

- Gradient on Blackhawk Island, Wisconsin.” *Ecology* 65 (1): 256–68.  
doi:10.2307/1939478.
- Pennington, P. I., and R. C. Ellis. 1993. “Autotrophic and Heterotrophic Nitrification in Acidic Forest and Native Grassland Soils.” *Soil Biology and Biochemistry* 25 (10): 1399–1408. doi:10.1016/0038-0717(93)90054-F.
- Perakis, Steven S., Jana E. Compton, and Lars O. Hedin. 2005. “Nitrogen Retention across a Gradient of 15N Additions to an Unpolluted Temperate Forest Soil in Chile.” *Ecology* 86 (1): 96–105. doi:10.2307/3450991.
- Pérez, Cecilia A., Lars O. Hedin, and Juan J. Armesto. 1998. “Original Articles: Nitrogen Mineralization in Two Unpolluted Old-Growth Forests of Contrasting Biodiversity and Dynamics.” *Ecosystems* 1 (4): 361–73.  
doi:10.1007/s100219900030.
- Persson, Hans, Hooshang Majdi, and Anna Clemensson-Lindell. 1995. “Effects of Acid Deposition on Tree Roots.” *Ecological Bulletins*, no. 44 (January): 158–67.  
doi:10.2307/20113159.
- Persson, T., and A. Wirén. 1995. “Nitrogen Mineralization and Potential Nitrification at Different Depths in Acid Forest Soils.” *Plant and Soil* 168-169 (1): 55–65.  
doi:10.1007/BF00029313.
- Piatek, Kathryn B., and Mary Beth Adams. 2011. “Are Nitrate Exports in Stream Water Linked to Nitrogen Fluxes in Decomposing Foliar Litter?” In *Proceedings of the 17th Central Hardwood Forest Conference*, 5–7.  
<http://www.treearch.fs.fed.us/pubs/38050>.

- Shenk, Gary W., and Lewis C. Linker. 2013. "Development and Application of the 2010 Chesapeake Bay Watershed Total Maximum Daily Load Model." *JAWRA Journal of the American Water Resources Association* 49 (5): 1042–56. doi:10.1111/jawr.12109.
- Simmons, Jeffrey A., William S. Currie, Keith N. Eshleman, Karen Kuers, Susan Monteleone, Tim L. Negley, Bob R. Pohlad, and Carolyn L. Thomas. 2008. "Forest to Reclaimed Mine Land Use Change Leads to Altered Ecosystem Structure and Function." *Ecological Applications* 18 (1): 104–18. doi:10.1890/07-1117.1.
- Stone, K.M., and E.D. Matthews. 1974. "Soil Survey of Allegany County, Maryland". United States Government Printing Office. Document 0-478-938, Washington, DC.
- Tsunogai, U., D. D. Komatsu, S. Daita, G. A. Kazemi, F. Nakagawa, I. Noguchi, and J. Zhang. 2010. "Tracing the Fate of Atmospheric Nitrate Deposited onto a Forest Ecosystem in Eastern Asia Using  $\delta^{17}\text{O}$ ." *Atmospheric Chemistry and Physics* 10 (4): 1809–20. doi:10.5194/acp-10-1809-2010.
- Vitousek, Peter M., James R. Gosz, Charles C. Grier, Jerry M. Melillo, William A. Reiners, and Robert L. Todd. 1979. "Nitrate Losses from Disturbed Ecosystems." *Science* 204 (4392): 469–74. doi:10.1126/science.204.4392.469.
- Waller, Kristin, Charles Driscoll, Jason Lynch, Dani Newcomb, and Karen Roy. 2012. "Long-Term Recovery of Lakes in the Adirondack Region of New York to Decreases in Acidic Deposition." *Atmospheric Environment* 46 (January): 56–64. doi:10.1016/j.atmosenv.2011.10.031.

Williard, Karl W. J., David R. DeWalle, Pamela J. Edwards, and Ronald R. Schnabel.

1997. "Indicators of Nitrate Export from Forested Watersheds of the Mid-Appalachians, United States of America." *Global Biogeochemical Cycles* 11 (4): 649–56. doi:10.1029/97GB01627.

Wright, Richard F., Erik Lotse, and Arne Semb. 1993. "RAIN Project: Results after 8

Years of Experimentally Reduced Acid Deposition to a Whole Catchment."

*Canadian Journal of Fisheries and Aquatic Sciences* 50 (2): 258–68.

doi:10.1139/f93-030.